IN-PLACE EFFICIENCY TESTS OF A LARGE SCALE VENTILATION EXHAUST FILTER*

B. J. Grady, Jr.** and K. H. Henry
Atlantic Richfield Hanford Company
Richland, Washington

Abstract

The in-place efficiency of the main ventilation system exhaust filters now in use at the Hanford Purex Plant has recently been determined by three independent test methods. Comparative evaluations of the test methods employed and their corresponding results have been made.

I. Introduction

The Hanford Purex Plant is used for the chemical reprocessing of irradiated nuclear fuels to recover and purify uranium, plutonium, and neptunium as products. Feed solution for solvent extraction processing is prepared by selective dissolution of the fuel element cladding material and subsequent dissolution of the irradiated uranium metal core in nitric acid. Several solvent extraction cycles, employing an organic tributyl phosphate solvent in normal paraffin hydrocarbon diluent, are used to separate the uranium, plutonium, and neptunium from one another and from fission product contaminants.

Due to the large amounts of radioactivity associated with the materials processed, the Purex Plant was built with massive concrete shielding between processing equipment and operating personnel. Thus most of the processes are operated remotely; that is, the basic operations, including much of the plant maintenance work, are controlled from remote stations, with no direct personnel observation of or contact with processing equipment.

Due to the nature of the materials processed, the operations conducted, and the remote processing equipment, it is to be expected that a slight amount of radioactive material will escape from process vessels. Almost any of the radionuclides present in the fuels processed may be associated with particulate matter and become airborne. Therefore, environmental and personnel protection concerns require that off-gases and ventilation exhausts from areas of potential radioactive contamination pass through high-efficiency air filtration systems for particulate matter removal.

II. Ventilation System Description

The Purex Plant building is a long, narrow concrete structure, 1,005 feet long, 119 feet wide at its widest point, and extending 64 feet above grade. The building consists of a heavily shielded concrete portion which contains the highly radioactive processing equipment, a pipe, sample, and storage gallery section, and a steel-and-transite annex housing the building services. The heavily shielded, or canyon, portion of the building

*Work performed under USAEC Contract AT(45-1)-2130
**Mr. Grady is now employed by Argonne National Laboratory at Idaho Falls, Idaho

extends about 40 feet below grade and is subdivided into a row of process equipment cells. The "hot" pipe trench, containing piping for radioactive solution transfers, and the ventilation air tunnel are adjacent to the canyon cells. The space above the canyon and hot pipe trench cover blocks contains the craneways for two gantry-type maintenance cranes. The gallery areas, arranged vertically adjacent to the canyon, primarily contain non-radioactive chemical piping to the cells, samplers for obtaining small-volume radioactive samples, and storage space for dry chemicals, spare equipment, and other supplies. Offices, locker rooms, electrical switchgear, operating control rooms, and aqueous chemical makeup facilities are located in the steel-and-transite portion of the building. A typical cross-section view of the concrete portions of the building is incuded in Figure 1.

The Purex Plant building ventilation systems are designed to minimize the personnel hazard of airborne radioactive particles. The basic philosophy behind ventilation system deisgn and operation is that differential air pressures shall be maintained between the various zones to assure that normal work areas are free of potentially contaminated air from special hazard zones. Thus, an air pressure balance is maintained such that the ventilation air flow between areas is from zones of least contamination toward more highly contaminated zones, that is, toward the canyon cells.

A schematic diagram of the canyon ventilation supply and exhaust systems is shown in Figure 1. Air drawn from outside the building is filtered, water-washed, humidified, heated, and delivered by supply fans to ducts located above the craneway. This air flow is automatically controlled by modulating dampers to maintain the desired absolute air pressure above the canyon cover blocks. Air enters the canyon cells through the crevices surrounding the cover blocks and exits the canyon through ventilation slots near the bottom of the canyon wall leading to the air tunnel. The air tunnel discharges through a large rectangular duct to two glass fiber filter beds operated in parallel. The filtered air is withdrawn by exhaust fans which discharge to the main 200-foot stack. Air flow through the exhaust fans is automatically controlled by modulating dampers to maintain the desired absolute air pressure in the air tunnel.

III. Filter Description

The two glass fiber filter beds are quite similar in design. Although each filter bed was designed to handle the entire 120,000 scfm air flow, the two units are currently being operated in parallel. The normal pressure drop for each filter bed is about two inches water gauge. Each filter bed is enclosed below grade in a concrete housing 82 feet long by 52 feet wide by 13 feet high and is divided into two areas, with one containing a fore-filter and the other an after-filter. The larger fore-filter portions remove most of the particulates from the incoming exhaust air; the smaller after-filter sections remove the fine particles which pass through the fore-filters. The major difference between the two filter bed units is that the fore-filter air flow direction is downflow for the original, or No. 1, filter and upflow for the new, or No. 2 filter. Air flows upwards through the after-filter sections of both units. Figure 2 shows a cut-away view of the No. 1 filter; the No. 2 filter is quite similar in appearance.

The fore-filter section of the No. 1 filter is divided into three bays containing seven-foot deep beds of free-packed Owens-Corning Fiberglas[R1], type 115K, retained by upper and lower stainless steel screens. The filter density gradient is calculated to range from 0.7 lb/ft^3 at the top to 3.3 lb/ft^3 at the bottom. The fore-filter section contains approximately 37,000 pounds of fibrous glass in 2,500 ft^2 of flow area.

The fore-filter section of the No. 2 filter is also divided into three bays containing seven-foot deep beds of Owens-Corning Fiberglas[R1], type 115K. However, the beds, rather than being free-packed, consist of five separately-supported packed layers. Starting at the bottom (fore-filter inlet), there are two 15-inch fiberglass layers at a free density of about 0.7 lb/ft^3, two 18-inch layers at a packed density of 1.5 lb/ft^3, and a final 18-inch layer at a packed density of 3.0 lb/ft^3.

The after-filter sections of both filter units are each made up of 132 American Air Filter Company Deep-Bed filter units. Each unit is packed with one-half inch of No. 25 FG Filterdown [R2] (1.4 lb/ft^3 density) followed by one-half inch of No. 50 FG Filterdown (1.2 lb/ft^3 density). The units consist of five wedge-shaped pockets supported in a grid on frames, as shown in Figure 2. There is a total of about 6,600 ft^2 of filtration area in each after-filter section.

IV. In-Place Filter Efficiency Tests

General Method

In early 1971 a program was initiated to determine the efficiency of the Purex Plant main ventilation exhaust filters. The basic test approach consisted of the introduction of an aerosol into the exhaust air upstream of the filters and the measurement of resulting aerosol concentration upstream of the filtration system and downstream of each filter unit. The test aerosol was introduced into the west branch of the air tunnel at a point about 200 feet upstream from the juncture of the east and west branches. The filter inlet aerosol measurements were made on samples withdrawn from a sample station located about 100 feet downstream from this juncture. Thus, it was believed that sufficient air-aerosol mixing was achieved prior to the filter inlet measurement. The two filter discharge sampling points were approximately 15 feet downstream from the respective filter units. In some instances the composite efficiency of both filters was verified by sampling from the short length of duct between the exhaust fans servicing both filters and the main 200-foot stack.

Sodium Aerosol Test

Three efficiency tests of the new, or No. 2, exhaust filter were conducted using a sodium aerosol generator and condensation nuclei counter. The sodium nuclei generator used to supply the test aerosol operated by bubbling compressed

R_1 Registered Trade Name, Owens-Corning Glass Co., Toledo, Ohio

R_2 Registered Trade Name, American Air Filter Co., Louisville, Kentucky

air into a saline solution and drawing a sample of the resulting salt entrained in air past an acetylene burner tip located in an open-ended cylinder. The sodium nuclei thus generated were introduced into the air tunnel aerosol inlet point, where they mixed with other nuclei already present in the air stream. In the condensation nuclei counter the air samples were passed through a chamber containing supersaturated water vapor, where the particles act as condensation nuclei and form small droplets. The counter readout is a function of the intensity of light scattered by the microscopic water droplets onto a photomultiplier tube. The background nuclei concentrations in the outside air and in the air tunnel were also determined at frequent intervals to check for changing background conditions. The statistical analysis of the test results is presented in the following table:

Test No.	No. 2 Exhaust Filter Efficiency (95 Percent Confidence Level)
1	98.90 ± 0.68
2	98.98 ± 0.42
3	99.39 ± 0.27
Average	99.09 (particle size assumed to be about 0.5 micron)

Certain problems, inherent in the particular test method and equipment used, caused the calculated filter efficiency to be less than expected. The nuclei counter is not specific for sodium nuclei and can detect a wide range of particle sizes, down to about 0.001 micron. It was observed that the background nuclei concentration in the filter exhaust samples was greater than one-half of that obtained during sodium nuclei testing. The ungenerated particles, which were not under experimental control, apparently cause a large variation with time in the filter effluent nuclei concentration. The source of the ungenerated particles was felt to be the outside air, since its nuclei concentration was found to vary considerably and roughly in parallel with the filter effluent nuclei concentration.

Fluorescein Aerosol Test

Three efficiency tests were performed on both ventilation exhaust filters utilizing a fluorescein aerosol generator and millipore collection filters. The fluorescein dye is the organic acid of the sodium salt, uranine, and has very similar properties. The fluorescein aerosol, produced by an atomizer-impactor generator, was introduced into the air tunnel at the same point used during the sodium nuclei testing. Filter inlet and exhaust samples were continuously withdrawn and passed through millipore filters to collect the fluorescein aerosol. The sample filters were washed with distilled water in the laboratory and the fluorescences of the resulting fluorescein solutions were measured with a calibrated fluorometer. During each test run a portion of the fluorescein aerosol was passed through a cascade impactor for particle size determination. Background levels of fluorescences were also determined prior to the first two runs.

The results of the fluorescein tests are summarized in the following table:

	Efficiency of Exhaust Filters (Percent)		
Test No.	Old (No. 1)	New (No. 2)	Mass Mean Particle Diameter (Microns)
1	>99.94	>99.92	0.43
2	>99.61	>99.42	0.30
3	>99.81	>99.27	0.30
Average	>99.79	>99.50	0.34

The slightly lower measured efficiencies in tests 2 and 3 were attributed to lower fluorescein concentrations in the filter inlet air, which would cause small differences in the outlet concentrations to be magnified, and to a slightly reduced particle size. Due to the No. 2 filter exhaust sample location used during the fluorescein tests, the values shown represent the efficiency of the fore-filter portion only. The "greater than" efficiency values were calculated conservatively by assuming that any measurable fluoresence extracted from filter exhaust samples is attributable to fluorescein particles which had penetrated the filters.

Dioctylphthalate (DOP) Aerosol Test

A series of five efficiency tests of the main ventilation exhaust filters were performed using a dioctylphthalate (DOP) aerosol. The aerosol was thermally generated from liquid DOP, using a developmental model high volume DOP generator, such that the resulting aerosol was polydisperse with a mass mean particle diameter of about 0.7 micron. During the DOP testing, which was performed during a plant shutdown period, canyon cell cover blocks at the west end of the building were removed to cause about 90 percent of the total air flow to pass through the west portion of the air tunnel, into which the DOP was introduced. This action provided increased assurance of adequate aerosol-air mixing prior to sampling. The experimental DOP generator allowed attainment of a filter inlet DOP concentration of about 32 miligrams per cubic meter in a total air flow of slightly over 120,000 CFM. The DOP concentrations in filter inlet and exhaust air samples were determined by two forward light-scattering photometers which were calibrated together at the filter inlet sampling point. The test series included an additional sampling point, located in the short length of duct between the exhaust fans and the stack, to provide a direct measure of combined filter efficiency.

The results of the DOP testing are shown in the following table:

Test No.	Filter Bank	Efficiency, Percent
1	No. 1	99.74
2	No. 1	99.73
3	No. 2	99.64
4	No. 2	99.68
5	No. 1 & No. 2	99.60

V. Summary and Conclusions

The fluorescein and DOP tests were found to produce acceptable results that were in close agreement. It was felt that the fluorescein aerosol test possessed some operational advantages over the DOP aerosol method in that relatively less elaborate aerosol generation and sampling equipment were required. The sodium nuclei test failed to produce acceptable results due to the combined problems of varying background particle concentration and low sodium nuclei generation rate. Additional development of sodium nuclei generators for large scale applications could perhaps resolve these problems.

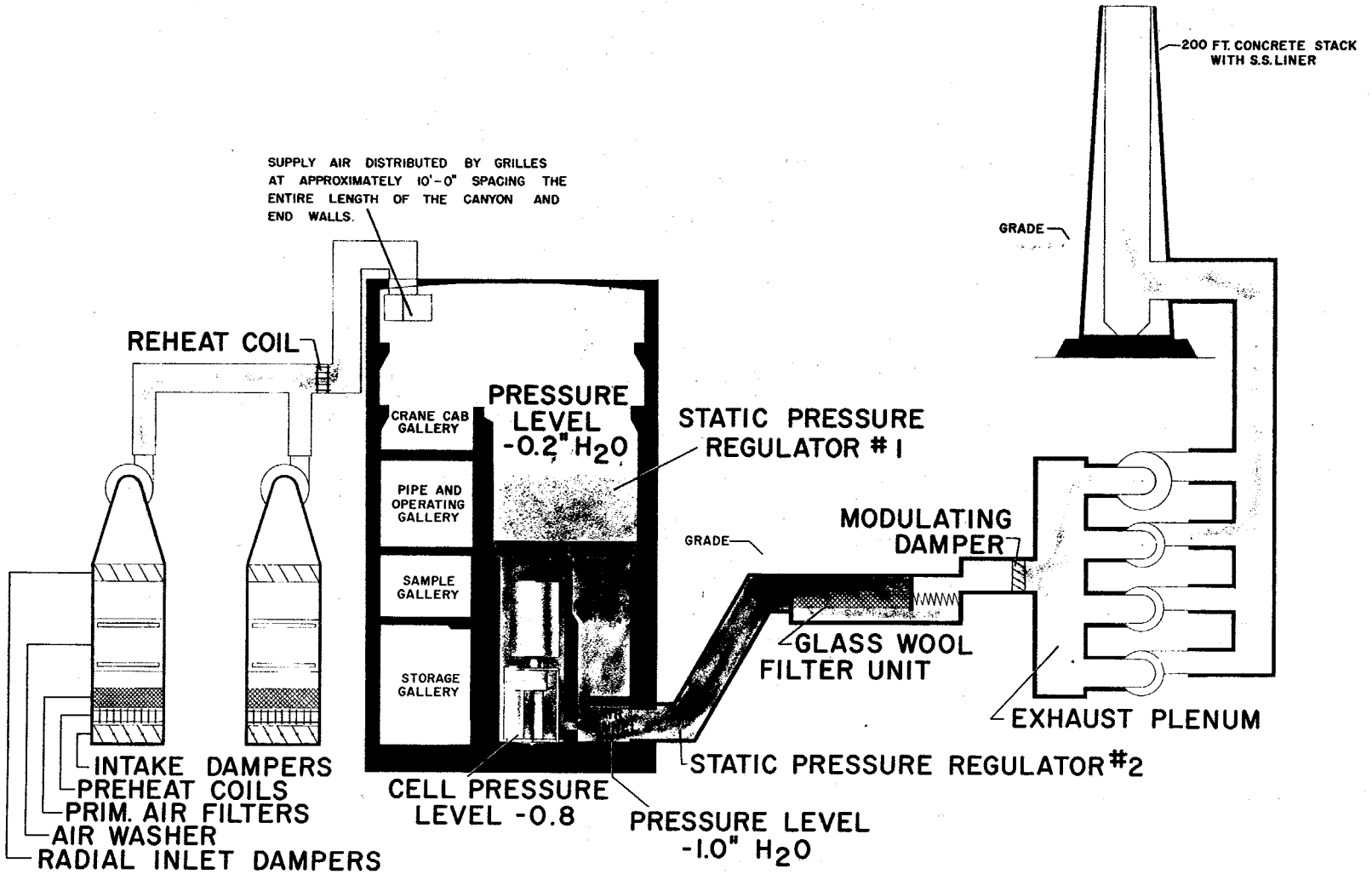

Figure 1

Process Area Ventilation System

AEC-RL RICHLAND, WASH.

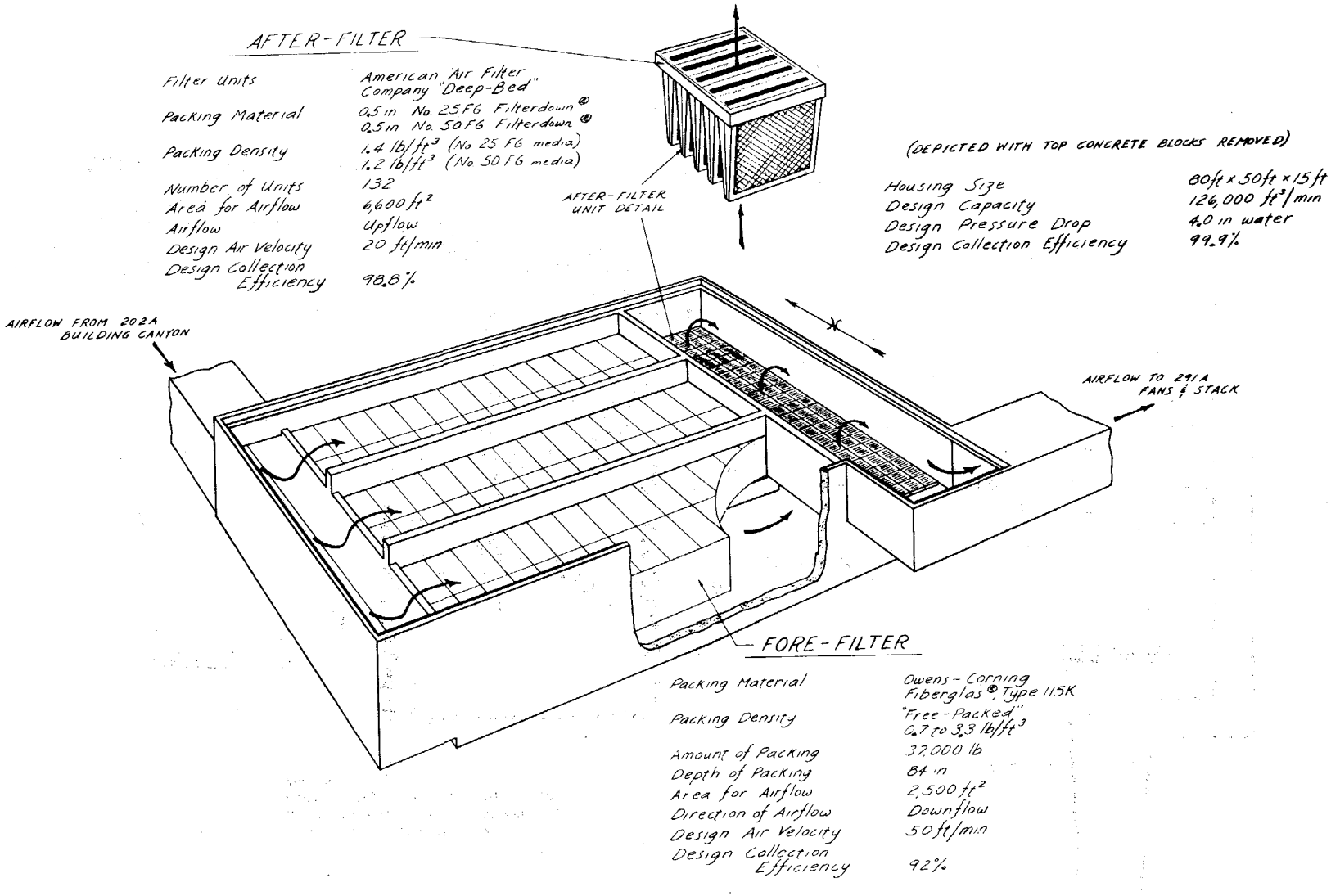

FIGURE 2

291-A Filter No. 1

DISCUSSION

STAFFORD: By using polydisperse DOP aerosol you have selective impaction of large particles on the face of the filter. This produces two aerosols, the upstream aerosol and down-stream aerosol, each with different size characteristics. Since forward light scatter is an exponential function of particle size, would you anticipate that there could be errors in your filter efficiency calculations by light scatter with polydispersed aerosol, and, if so, how large could this error be?

HENRY: I am not sure I know the answer to that question. Mr. Gil Rolie, who is presenting a paper later, assisted us with these tests and I feel that might be a question that he would be better able to answer than I. Perhaps you could ask him at that time.

CRAIG: My question goes somewhat along the same line, but I want to ask it in two parts. First, what sort of cascade impactor did you use for your size distribution test; second, did you take samples downstream of the filter and, if so, what were the results?

HENRY: To answer your second question first, we did not use a cascade impactor on filter exhaust samples.

GRADY: In answer to your first question, we used the Scientific Advances cascade impactor.

EFFECTS OF RADIATION ON REACTOR CONFINEMENT SYSTEM MATERIALS*

L. R. Jones
Savannah River Laboratory
E. I. du Pont de Nemours and Co.
Aiken, South Carolina 29801

Abstract

Materials for airborne-activity confinement systems are being irradiated by a ^{60}Co source at a rate of $\sim 4 \times 10^7$ rads/hr to simulate the performance characteristics of the materials following a reactor accident. In a reactor accident, radioiodine and radioactive particulates would accumulate in the confinement system and would produce an intense radiation field. The materials are being irradiated in a miniature confinement system containing a moisture separator, a HEPA filter, and a carbon bed in series. Single materials are also being irradiated. Test facilities and qualitative measurements of changes in pertinent material properties during irradiation are described.

On November 9, 1970, about 85,000 curies of particulate activity was released into the K reactor room from an irradiated antimony-beryllium source rod that melted while suspended in air. Approximately 6247 curies reached the confinement filters; only 3 millicuries escaped to the environs. Inspection of contaminated filter components for radiation damage is described.

Introduction

In the highly unlikely event of a major reactor accident, radioiodine and radioactive particulates would accumulate on filter and adsorber units in the airborne-activity confinement system. The radiation intensity produced by this accumulated radioactivity could be sufficient to damage confinement system components or alter their performance following the accident. Radiation effects on component materials are being measured at the Savannah River Laboratory (SRL) as part of a continuing program in support of reactor confinement facilities at the Savannah River Plant (SRP)[1-10]. Effects of gamma radiation on adsorption of iodine on activated carbon are reported in other SRL reports[10,11]. This paper reports effects of radiation on other confinement system component materials such as particulate (HEPA) filter media, moisture separator (demister) media, and gasket and adhesive materials.

* The information contained in this article was developed during the course of work under Contract AT(07-2)-1 with the U. S. Atomic Energy Commission.

Facilities and Techniques

^{60}Co Irradiation Facility

The SRL ^{60}Co Irradiation Facility includes three ^{60}Co sources. Two smaller sources are permanently positioned around the base of two 6-inch-diameter air-filled access tubes. One larger source can be positioned in several locations where samples are to be irradiated. Each of the smaller sources consists of ∿0.25 megacurie of ^{60}Co (on Jan. 1, 1972) contained in 22 slugs in a slug holder positioned at the base of each access tube. The larger source consists of 1.64 megacuries of ^{60}Co (on Jan. 1, 1972) contained in 28 slugs in a movable slug holder.

Approximately 24 feet of water provide shielding and cooling for the sources. Mechanical and procedural restraints prevent the movable source from being raised far enough from the floor of the water pit to significantly reduce shielding. A heat exchanger and filter system maintain water clarity and remove ∿32 kilowatts of heat produced from ^{60}Co decay.

The larger source can be used for static or dynamic tests. For static tests the source is positioned around a storage rack located on the floor of the water-filled pit which houses the facility. Located in the center of the source (Figure 1) is the sample irradiation container used for static material irradiations. The container is purged continuously with dry air during irradiation, and temperature is monitored. Figure 2 shows the irradiation container disassembled following irradiation of neoprene sponge gasket samples.

For dynamic tests, the large 10-inch-diameter air-filled access tube shown in Figure 1 is used. Figure 3 shows the source positioned around the base of the 10-inch access tube. The slug holder is constructed in two halves which are hinged so that the assembly can be opened and closed around the tube.

The Confinement System Irradiation Test Section for dynamic tests is shown in Figure 4. Samples of moisture separator material, HEPA filter media, activated carbon, and gasketing material are irradiated while subjected to conditions of flow, temperature, humidity, and iodine loading, which might be expected following a major reactor accident. A detailed description of this apparatus is given in Reference 11 with activated carbon performance data. Performance of other materials in this apparatus was examined for comparison with static irradiation results. Moisture separator samples receive ∿6 hours exposure time in a gamma field of $\sim 3 \times 10^6$ rad/hr while HEPA filter samples and gasket material receive the same exposure time in a field of $\sim 3 \times 10^7$ rad/hr during a normal system test. The HEPA filter samples are exposed to a higher dose rate than the moisture separators because they are located at about the same elevation as the ^{60}Co slugs.

Material Property Measurements

Changes in material properties were measured both at SRL and at the Naval Research Laboratory (NRL) in Washington, D.C. Tensile strength tests, DOP penetration, dry air flow resistance, weight per unit area, moisture and combustible content, and thickness measurements on HEPA filter media were made at NRL.

Relative measurements of water repellency and wet strength of HEPA filter media were made at SRL. Each sample of media was clamped between two flanges containing 2-inch-diameter holes. Alignment of these holes left a 2-inch-diameter area of the sample media exposed and unsupported on either face. A 6-inch column of water was then supported by the exposed media until a drop of water penetrated the media. The time required for water to penetrate the media was taken as a measure of relative water repellency.

Immediately following penetration of the first drop of water through the media, the water column height was increased at the rate of 1 inch every 5 seconds until the media ruptured. The height of the water column required to rupture the media was taken as a measure of relative wet strength.

Three-inch-diameter samples of HEPA filter media were also exposed to flow of saturated air (dew point 30°C) at a face velocity of 3 ft/min for 8 hours to observe blinding of the media as a function of flow exposure time.

Shore hardness of gasketing materials was measured with a "Clarkstan" rubber hardness gauge.

Components Contaminated in Source Rod Incident

Beta and gamma radiation exposure to filter components in the K reactor confinement system resulted from trapping antimony and tellurium activity released from an antimony-beryllium source rod which melted while suspended in air in the K reactor room on November 9, 1970. A detailed description of this incident is reported in Reference 12. On March 21, 1972, samples of moisture separator media, HEPA filter media, and activated carbon were removed from the most highly contaminated of the four confinement compartments and examined for radiation degradation.

Water repellency tests were run on samples of the contaminated filter media. Samples of contaminated moisture separator media were irradiated in the ^{60}Co irradiation facility simultaneously with used moisture separator media having no incident history, and a degradation comparison was made. The calculated radiation dose rates to demisters and HEPA filters at the time of the incident (November 9, 1970) and integrated radiation doses (∿80% beta, 20% gamma) to May 1, 1972 are shown in Table I. Isotopic activities were calculated from radiation measurements from filter samples. It was assumed that 100% of the beta energy and 5% of the gamma energy was absorbed in filter component materials.

Results

Filter Construction Materials

Two samples of asbestos HEPA filter separator material were exposed to ∿5 x 10^7 rads in a 1.7 x 10^7 rad/hr gamma field and are shown in Figure 5 (bottom row). Unirradiated materials are also shown for comparison (top row). No changes in material appearance or color were observed after irradiation. Physical properties

of the materials were measured at NRL before and after irradiation and are summarized in Table II. None of the properties measured, except for moisture content, were significantly affected by the radiation exposure.

Samples of rubber-base and foam adhesives used in the construction of HEPA filters were irradiated and are shown in Figure 6. Metal strips, 1 inch wide, were bonded together with each type of adhesive. The bond strength of each adhesive was then measured at NRL on samples with no radiation exposure and on samples which had been exposed to $\sim 5 \times 10^7$ rads in a 1.7×10^7 rad/hr gamma field. The samples in Figure 6 are shown following bond strength tests. Samples in the top row received no radiation exposure. Samples in the bottom row were irradiated. Bond strength data are shown in Table III.

Adhesives A and C showed darkening of color after irradiation. Adhesives B and C showed good bonding to surfaces, although adhesive C lost some bond strength. Adhesive A showed no bonding after irradiation and separated easily from the metal surface as shown in Figure 6.

Samples of plywood and particle board supplied by AEC Division of Operational Safety of the type used as framing material for some HEPA filters were exposed to $\sim 5 \times 10^7$ rads in a gamma field of 1.7×10^7 rad/hr. Both materials appeared unchanged except for slight discoloration and bakeout of impregnant. Additional samples were exposed to $\sim 3 \times 10^9$ rads in a 4.5×10^7 rad/hr field. These irradiated materials became crumbly and brittle with darkening in color (Figure 7).

Gasketing Material

Sponge Neoprene

Samples of closed cell neoprene sponge of the type used to seal filters to installation frames were irradiated to various exposures in a gamma field of 4.5×10^7 rad/hr. Figure 8 shows an unirradiated sample (top) and an irradiated sample (bottom) exposed to 9×10^8 rads. The irradiated material showed extreme brittleness at this exposure and could be crumbled into small particles having the appearance of charcoal. Hardening of the material occurred at lesser exposures and is shown as Shore hardness in Figure 9. At exposures greater than $\sim 4 \times 10^8$ rads, hardness measurement caused permanent deformation of the material surface and was considered invalid.

A one-half-inch wide neoprene sponge gasket is used in the Confinement System Irradiation Test Section to simulate performance of gaskets which seal carbon beds in SRP confinement facilities. Several tests have been run in which this gasket was exposed to $\sim 3 \times 10^8$ rads prior to injecting iodine into the system. The efficiency of the system for removing iodine from the flowing air stream was consistent with the established efficiency of the activated carbon used indicating that no gasket leakage occurred. The gaskets were compressed to $\sim 50\%$ of their original thickness during these tests and were found to be permanently deformed following their irradiation.

Silicone Gasketing Grease

Because operating experience has shown that neoprene sponge gaskets deform permanently and lose their compressibility when tightly compressed for several months in filter installations, silicone gasketing grease has been suggested as a possible substitute for the sponge neoprene material. Two types of silicone grease

were irradiated in a gamma field of 4.5×10^7 rad/hr. Samples of the unirradiated greases (top) and samples exposed to 9×10^7 rads (middle) and $\sim 3 \times 10^9$ rads (bottom) are shown in Figure 10. Both types of grease showed hardening into a silicone rubber with extensive void formations. The formation of voids was a result of increasing the temperature of the material to ~140°C during irradiation because of gamma absorption. Heating the material in an oven to 140°C resulted in similar void formation, but no hardening. Increased exposure caused crystallization of both materials into a flakey powder resembling mica with slight darkening of color.

Shore Hardness

Figure 11 shows Shore hardness of both silicone greases as a function of gamma exposure. Inconsistencies in hardness measurements were caused by the voids in the material. Each data point in Figure 11 is an average value for four measurements made on a sample. At exposures greater than $\sim 1 \times 10^8$ rads, hardness measurement caused permanent deformation of the material surface and was considered invalid.

Moisture Separator Material

*Teflon**-Stainless Steel Demister

Samples of moisture separator material made of *Teflon*-coated stainless steel were irradiated to various exposures in a gamma field of 4.5×10^7 rad/hr. No degradation was observed at exposures less than 2×10^7 rads. Disintegration of the *Teflon* fibers was observed at greater exposures. Figure 12 shows a sample of unirradiated material (left) and a sample of material exposed to 2.4×10^8 rads (right). The *Teflon* fibers were shaken from part of the irradiated sample leaving only the stainless steel mesh.

Teflon-coated stainless steel material is used in the Irradiation Test Section to simulate performance of *Teflon*-stainless steel moisture separators in SRP confinement facilities. Tests have been run in which this material was exposed to $\sim 4 \times 10^7$ rads while a steam-air mixture at 80°C and 100% relative humidity flowed through the material. *Teflon* fibers were found in the condensate removed by the moisture separator from the flowing air stream, but no gross damage to the material was observed.

Teflon-stainless steel moisture separators in the K reactor confinement system received beta and gamma radiation doses shown in Table I from antimony and tellurium contamination. Based on these doses and exposure of unused material in the ^{60}Co gamma field, no damage to the K reactor moisture separators would be expected. Examination of the contaminated material showed no damage. Simultaneous irradiation in the ^{60}Co gamma field of contaminated material and uncontaminated material with normal service showed similar damage to both materials at exposures of 2×10^7 rads and 5×10^7 rads.

Glass Fiber Demister

Samples of a glass fiber moisture separator material were exposed to 2.4×10^8 rads in a 4.5×10^7 rad/hr gamma field. An unirradiated sample (left) and an irradiated sample (right) are shown in Figure 13. The glass fiber material appeared unaffected following the radiation exposure.

---

* Trademark of Du Pont Company, Wilmington, Del.

HEPA Filter Media

Static Irradiations

Samples of six glass fiber HEPA filter media, produced by different manufacturers or by different processes, were irradiated to various exposures in a gamma field of $\sim 4.5 \times 10^7$ rad/hr.

Water repellency of each media was measured as a function of gamma exposure as shown in Figure 14. Media A, B, and C deteriorated more rapidly than Media D, E, and F. Water penetration in 5 to 6 seconds was characteristic of complete loss of water repellency for all media. Media C showed poor water repellency even when unirradiated and gave inconsistent data indicating nonuniform waterproofing treatment. Samples with water penetration times of 60 to 100 seconds absorbed a drop of water placed on the surface of the media in 1 to 3 minutes depending on the media type. Samples with penetration times less than 10 seconds absorbed the water drop instantly.

Wet strength of each media was also measured as a function of gamma exposure and is shown in Figure 15. Irradiated samples were ruptured immediately following initial penetration of the sample by a drop of water as discussed previously. Data shown in Figure 15 at zero gamma exposure were measured in the same way except that these samples were ruptured with no water drop penetration. These data do not represent wet strength in the same sense as data for irradiated samples because the media was not wetted prior to rupture.

The media showed no change in appearance, except for slight yellowing of Media C. Other properties were measured before and after exposure to 5×10^7 rads for all media except E. Data shown in Table IV indicate a range of properties for the several commercial filter media tested. The results have not been related to differences in the products nor has a suitable performance index been established.

Simulated Accident Performance

Media E was used in the Irradiation Test Section to simulate performance of HEPA filters in SRP confinement facilities. A portion of media was exposed to $\sim 2.3 \times 10^8$ rads during a normal test, while other portions received less exposures because of the gamma field gradient across the HEPA filter module of the test section. Wetting of portions of the media in the greatest field has been observed following 100% relative humidity tests, but no rupture has occurred.

Media Contaminated During Source Rod Incident

HEPA filters in the K reactor confinement system received beta and gamma radiation doses shown in Table I from antimony and tellurium contamination. Based on these doses and exposure of unused HEPA media in the ^{60}Co gamma field, no damage to the K reactor HEPA filters would be expected. Water repellency of the contaminated media was measured and compared with water repellency of used media with longer service in SRP confinement facilities but with no contamination or incident history. The contaminated media showed some degradation of water repellency and wet strength, but the material with normal service was less water repellent than the contaminated media. Further testing of used media showed increased deterioration of SRP HEPA filters with increased service age. Water repellency data is shown in Table V. Degradation of the contaminated HEPA media is most likely a result of normal service exposure rather than radiation damage.

Normal Service Deterioration

Deterioration of HEPA filter media with normal service is being investigated. Behavior of used media exposed to flow of saturated air (dew point 30°C) is shown in Figure 16. Also shown for comparison are data on unused unirradiated media and unused media exposed to 1.8×10^8 rads in the ^{60}Co gamma field.

A black soot accumulates on HEPA filters as service in the confinement system increases. Blinding of used media with moisture during saturated air flow tests correlates closely with the quantity of soot deposited on the media. Deterioration of water repellency also correlates more closely with soot loading on the media than with actual service age. Behavior of media with 7 months and 48 months service is compared in Figure 16. The 7-month service media has a light soot loading and retains its water repellency as indicated by gradual blinding and no continuing increase in ΔP to rupture. The 48-month service media has a heavier soot layer and shows rapid blinding of the soot layer followed by blinding of the media and rupture.

Treatment of unused media with a solution of the black soot in ethyl alcohol destroyed the water repellency of the unused media. Treatment with alcohol alone had no effect and suggests that a contaminant in the soot may be reacting chemically with the waterproofing agent in the media. Chemical analysis of the soot is expected to identify contaminants that might react with the waterproofing agent.

Electron Microscope Examination

Figure 17 shows scanning electron microscopy photographs of unused unirradiated HEPA filter media (top row) and unused media exposed to 1×10^9 rads in a 4.5×10^7 rad/hr gamma field. The irradiated material appears to show some loss of binder between the glass fibers at a magnification of ∿600. At magnifications of 6000 and greater, small blisters can be observed on the surfaces of the glass fibers of the unirradiated media. No such blisters were observed on the irradiated material. The blisters may indicate a coating of waterproofing agent on the fibers. Lack of blisters in irradiated media may indicate an absence of waterproofing agent.

Figure 18 shows media with ∿48 months service in SRP confinement facilities. Both the upstream side of the media covered with the black soot layer (top row) and the downstream or clean side of the media (bottom row) are shown. The soot particles clearly appear to be attached to the surface coating of binder on the glass fibers and are small enough to migrate through the media. Simple migration and absorption of these hydrophylic particles may be creating a rough coating over the waterproofing agent thus rendering the media non-water-repellent to the depth of migration of the soot particles. No significant erosion of the binder from 48 months of air flow is apparent.

Summary

Asbestos HEPA filter separator materials irradiated in a ^{60}Co gamma field were not significantly affected by the radiation exposure. Two rubber-base HEPA filter adhesives showed adequate bond strength after irradiation while one foam adhesive showed complete loss of bonding ability. HEPA filter framing materials retained their integrity at exposures less than 10^8 rads but became brittle at greater exposures. Neoprene sponge gasketing material showed hardening and embrittlement at exposures greater than 4×10^8 rads. Silicone greases proposed as substitutes for the sponge neoprene material showed hardening and void formation at exposures less than 1×10^8 rads and crystallization at greater exposures. *Teflon*-coated

stainless steel used in moisture separators showed disintegration of *Teflon* fibers at exposures greater than 2 x 10^7 rads, while glass fiber demister material showed no damage. Glass fiber HEPA filter media showed degradation of water repellency and wet strength following irradiation. Some types of media were severely degraded at exposures of ~3 x 10^7 rads, while others required exposures greater than 2 x 10^8 rads for similar degradation.

Examination of components contaminated with antimony and tellurium activity in the K reactor confinement system showed no damage from beta and gamma radiation exposure at calculated exposures up to 6 x 10^6 rads. Deterioration of HEPA filters with normal service in SRP confinement facilities was found and is being investigated.

Acknowledgment

The author gratefully acknowledges the assistance of W. L. Anderson at the Naval Research Laboratory in preparation of this paper.

References

1. W. S. Durant, R. C. Milham, D. R. Muhlbaier, and A. H. Peters. *Activity Confinement System of the Savannah River Plant Reactors.* USAEC Report DP-1071, E. I. du Pont de Nemours & Co., Savannah River Laboratory, Aiken, S. C. (1966).

2. W. S. Durant. *Performance of Activated Carbon Beds in SRP Reactor Confinement Facilities - Progress Report: September 1961-September 1965.* USAEC Report DP-1028, E. I. du Pont de Nemours & Co., Savannah River Laboratory, Aiken, S. C. (1966).

3. R. C. Milham. *High Temperature Adsorbents for Iodine - Progress Report: January 1965-September 1966.* USAEC Report DP-1075, E. I. du Pont de Nemours & Co., Savannah River Laboratory, Aiken, S. C. (1966).

4. R. C. Milham and L. R. Jones. *Iodine and Noble Gas Retention Studies - Progress Report: October 1966-December 1968.* USAEC Report DP-1209, E. I. du Pont de Nemours & Co., Savannah River Laboratory, Aiken, S. C. (1969).

5. R. C. Milham and L. R. Jones. *Iodine Retention Studies - Progress Report: January 1969-June 1969.* USAEC Report DP-1213, E. I. du Pont de Nemours & Co., Savannah River Laboratory, Aiken, S. C. (1969).

6. R. C. Milham and L. R. Jones. *Iodine Retention Studies - Progress Report: July 1969-December 1969.* USAEC Report DP-1234, E. I. du Pont de Nemours & Co., Savannah River Laboratory, Aiken, S. C. (1970).

7. A. G. Evans and L. R. Jones. *Iodine Retention Studies - Progress Report: January 1970-June 1970.* USAEC Report DP-1259, E. I. du Pont de Nemours & Co., Savannah River Laboratory, Aiken, S. C. (1971).

8. A. G. Evans and L. R. Jones. *Iodine Retention Studies - Progress Report: July 1970-December 1970.* USAEC Report DP-1271, E. I. du Pont de Nemours & Co., Savannah River Laboratory, Aiken, S. C. (1971).

9. A. G. Evans and L. R. Jones. *Confinement of Airborne Radioactivity - Progress Report: January 1971-June 1971.* USAEC Report DP-1280, E. I. du Pont de Nemours & Co., Savannah River Laboratory, Aiken, S. C. (1971).

10. A. G. Evans and L. R. Jones. *Confinement of Airborne Radioactivity - Progress Report: July 1971-December 1971.* USAEC Report DP-1298, E. I. du Pont de Nemours & Co., Savannah River Laboratory, Aiken, S. C. (1972).

11. A. G. Evans. "Effect of Intense Gamma Radiation on Radioiodine Retention by Activated Carbon." *Proceedings of the Twelfth AEC Air Cleaning Conference,* Oak Ridge, Tenn., August 28-31, 1972.

12. J. W. Little, Jr. and J. W. Joseph, Jr. "Confinement of Airborne Activity from Melted Antimony Slugs." *Proceedings of the Twelfth AEC Air Cleaning Conference,* Oak Ridge, Tenn., August 28-31, 1972.

TABLE I

Filter Units Contaminated in Sb Source Rod Incident

β,γ Dose Rate and Integrated Dose

Confinement Compartment	Moisture Separators		HEPA Filters	
	rad/hr (11-9-70)	rads (5-1-72)	rad/hr (11-9-70)	rads (5-1-72)
K2	949	6.9×10^5	8270	6.0×10^6
K3	1011	7.3×10^5	8890	6.4×10^6
K5	97	7.1×10^4	847	6.1×10^5
K6	6.3	4.5×10^3	54	3.9×10^4

TABLE II

Separator Irradiation Summary

Separator	A		B	
Exposed gamma dose, rads	0	5×10^7	0	5×10^7
Basis weight, lb/3000 ft^2	185	182	225	220
Moisture content, wt %	3.0	2.6	3.6	2.2
Weight loss after combustion, wt %	16.5	17.0	16.1	16.3
Thickness, mils	11-13	11-13	16-18	16-18
Tensile strength of 1-inch wide strip in machine direction, lb	11	10	25	25
Tensile strength of 1-inch wide strip in cross direction, lb	30	28	37	36
Color	Brown	Brown	Grey	Grey

TABLE III

Adhesive Irradiation Summary

Adhesive	Bond Strength, lb*	
	0 rads	5×10^7 rads
A (Foam Type)	85.7	0
B (Rubber Base)	138	140
C	353	218

* Shear strength of a 1-inch-wide by 1-inch-long bond.

TABLE IV

HEPA Filter Media Irradiation Summary

HEPA Filter Media	A		B		C		D		F	
Exposed gamma dose, rads	0	$5x10^7$	0	$5x10^7$	0	$5x10^7$	0	$5x10^7$	0	$5x10^7$
Basis weight, lb/3000 ft^2	61.2	61.0	52.7	52.3	49.4	48.9	58.6	58.6	50.0	49.7
Moisture content, wt %	0.8	1.7	0.3	2.0	1.7	1.7	1.8	1.1	0.2	0.78
Weight loss after combustion, wt %	3.0	1.5	3.9	2.8	3.9	2.4	4.95	4.80	2.1	1.7
Thickness, mils	15.5	15.5	14	14	16	15.5	17	16	19.5	19.5
DOP penetration @ 14.2 cm/sec, %	0.008	0.012	0.018	0.022	0.023	0.024	0.028	0.030	0.017	0.018
Flow resistance @ 14.2 cm/sec, mm H_2O	39	39	37	36	36	32	35.5	36	34.5	35
Tensile strength of 1-inch-wide strip in machine direction, lb	5.5	2.9	7.7	3.5	3.7	2.2	4.3	3.6	7.3	6.2
Tensile strength of 1-inch-wide strip in cross direction, lb	3.2	2.1	3.2	2.1	2.8	1.0	3.1	3.0	4.0	3.0

TABLE V

Water Repellency of Media with Service in SRP Confinement System

Service, months	Time for H_2O to Penetrate Media	Height of H_2O Column Required to Rupture Media, inches
Unused	>48 hr	39.5
4	>4 hr	32.5
7	>4 hr	28.0
11	209 sec*	6.7*
13	66 sec*	15.0*
48	57 sec*	10.4*

* Average of 10 tests

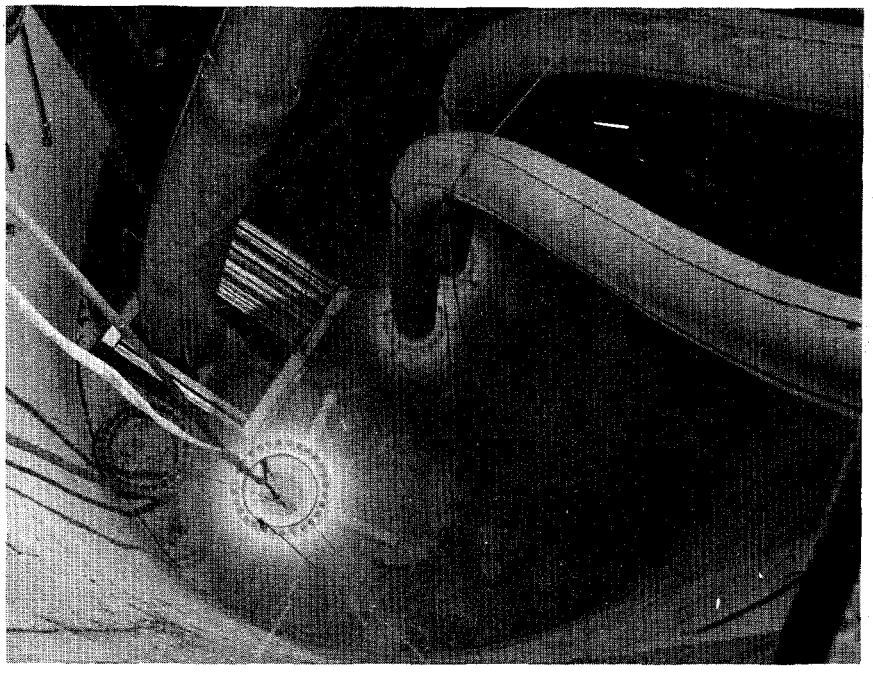

FIGURE 1. ^{60}Co SOURCE AND WATER PIT FACILITY

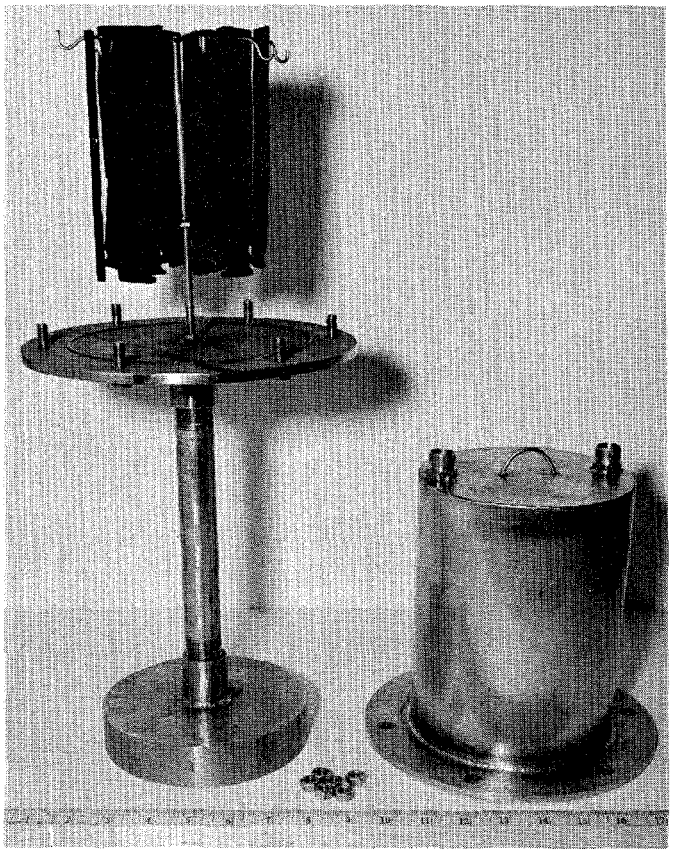

FIGURE 2. IRRADIATION CONTAINER WITH GASKET SAMPLES

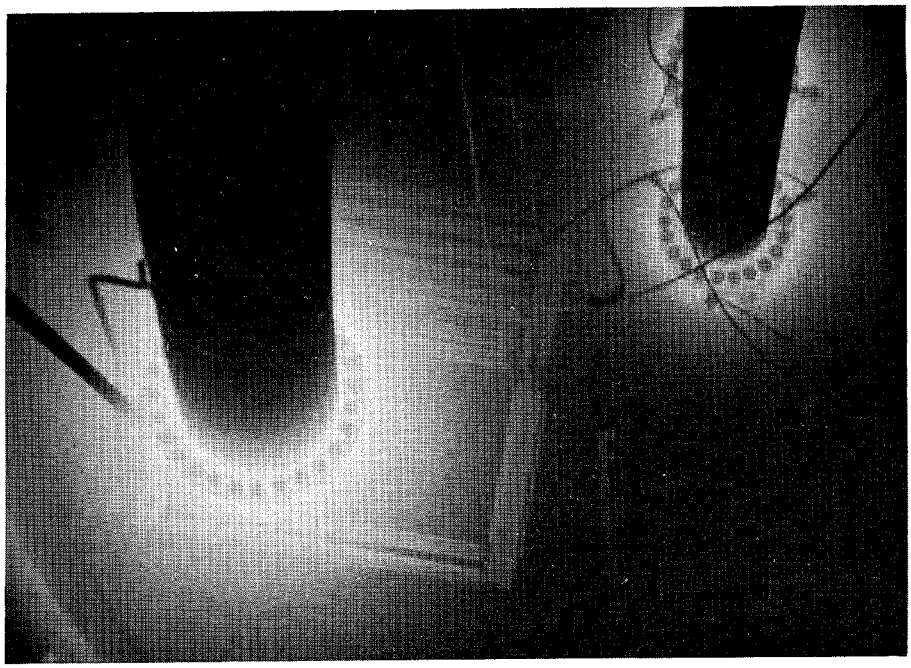

FIGURE 3. ^{60}Co SOURCE AROUND ACCESS TUBE

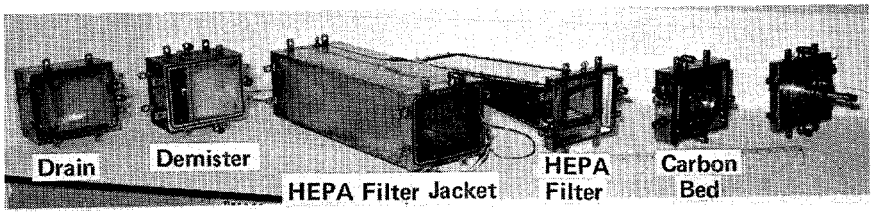

FIGURE 4. CONFINEMENT SYSTEM IRRADIATION TEST SECTION

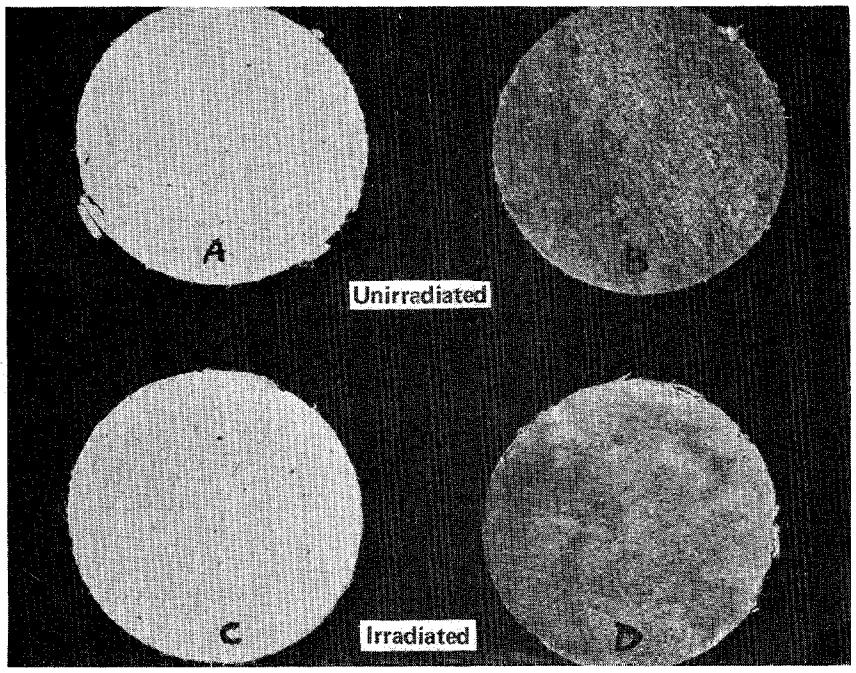

FIGURE 5. SEPARATOR MATERIAL

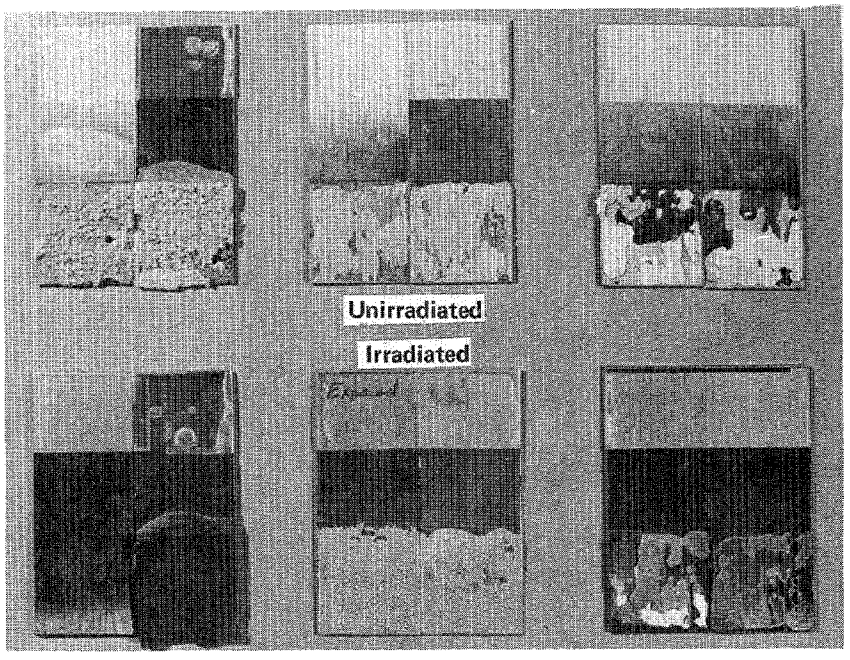

FIGURE 6. ADHESIVE SAMPLES

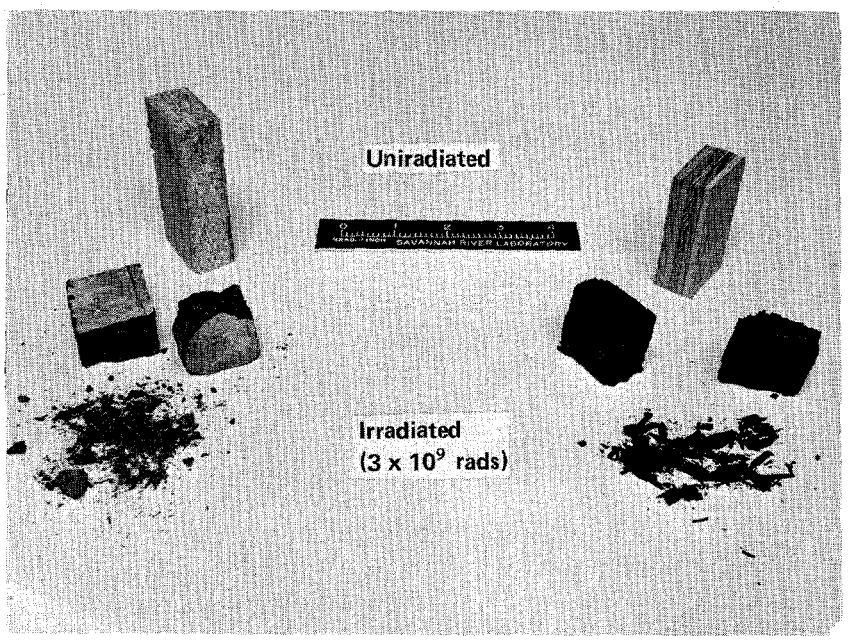

FIGURE 7. FRAMING MATERIALS

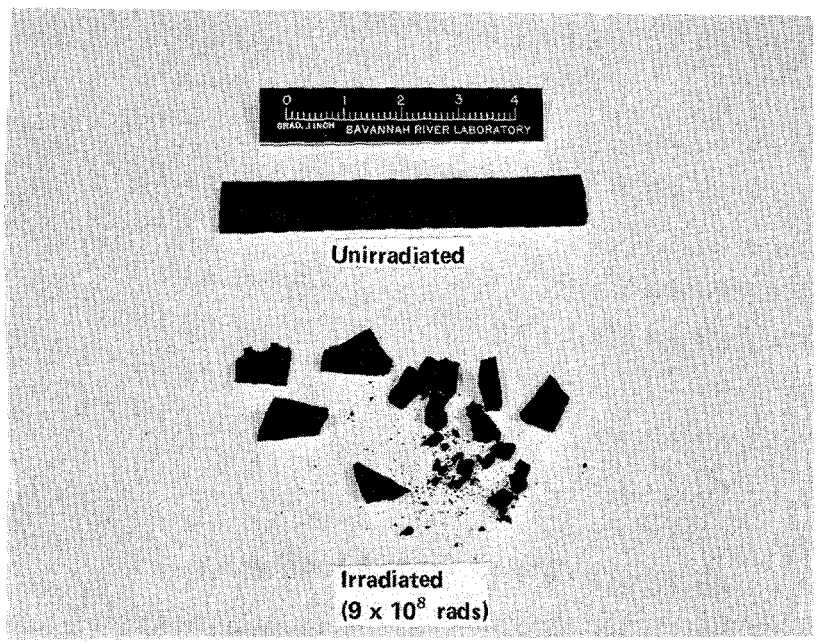

FIGURE 8. NEOPRENE SPONGE GASKET SAMPLES

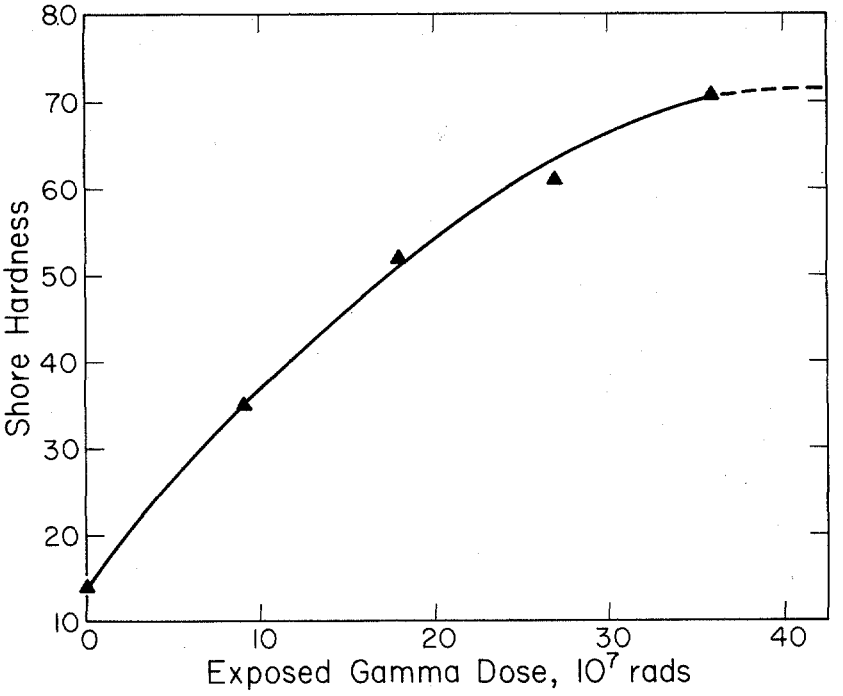

FIGURE 9. SHORE HARDNESS OF SPONGE NEOPRENE GASKET VS EXPOSED GAMMA DOSE

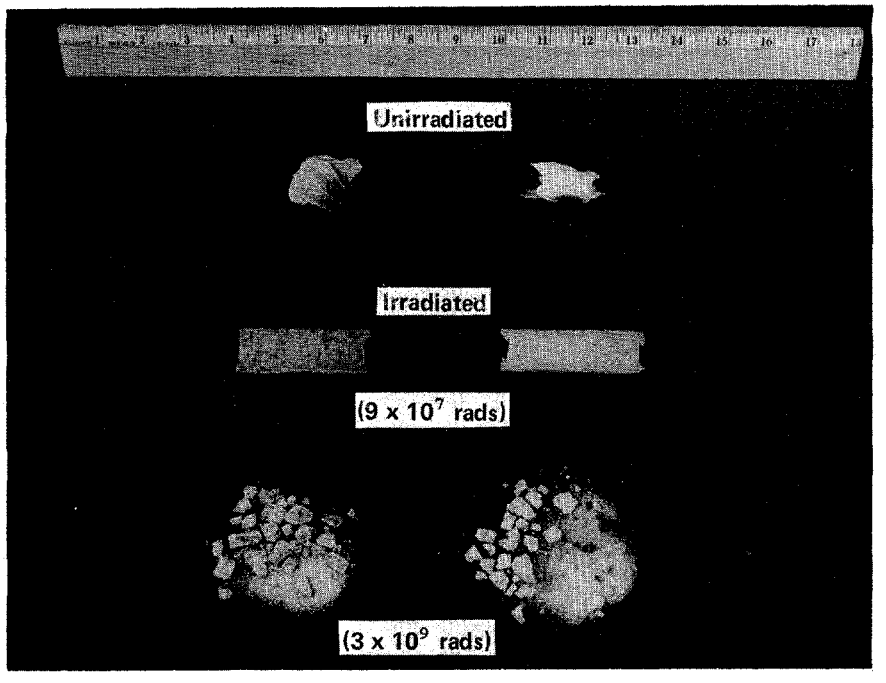

FIGURE 10. SILICONE GREASE SAMPLES

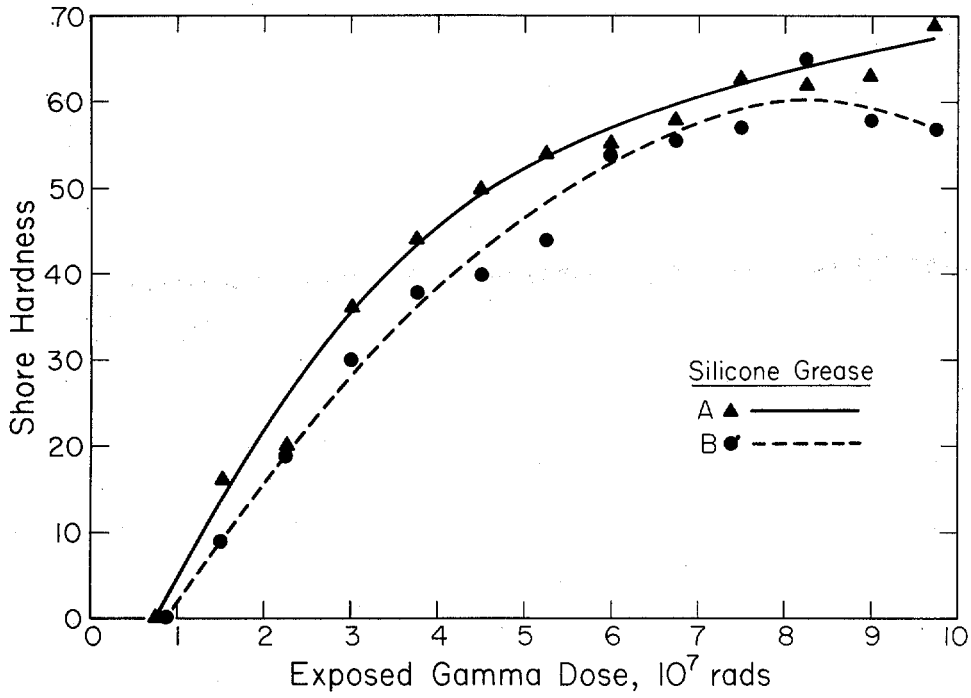

FIGURE 11. SHORE HARDNESS OF SILICONE GASKETING GREASE VS EXPOSED GAMMA DOSE

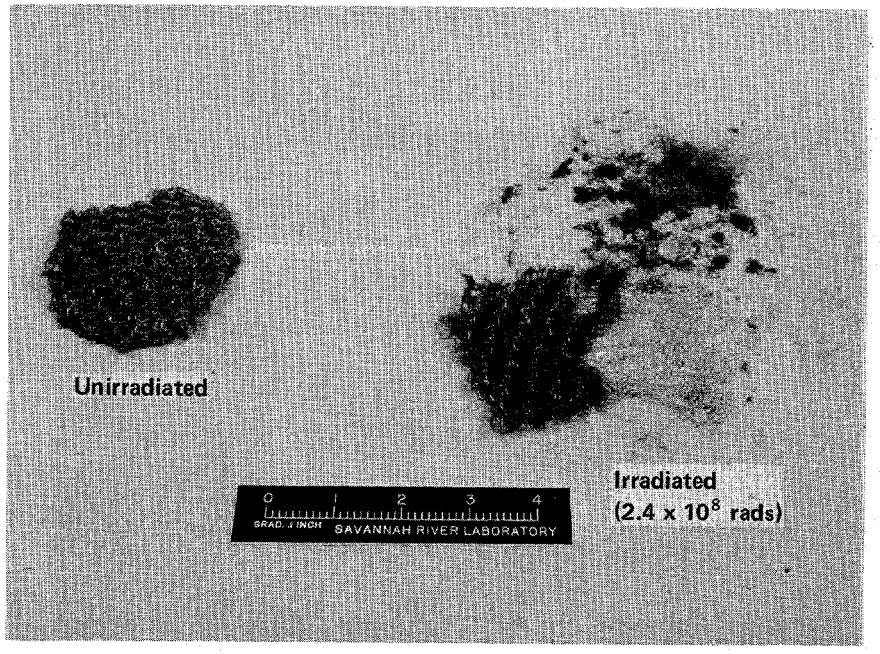

FIGURE 12. *TEFLON* AND STAINLESS STEEL DEMISTER MATERIAL

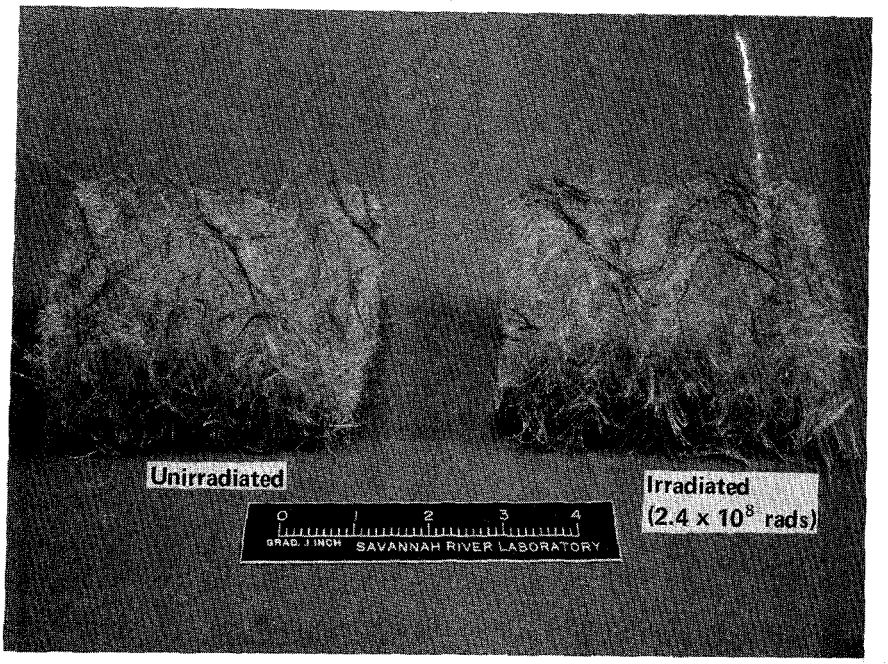

FIGURE 13. GLASS FILTER DEMISTER MATERIAL

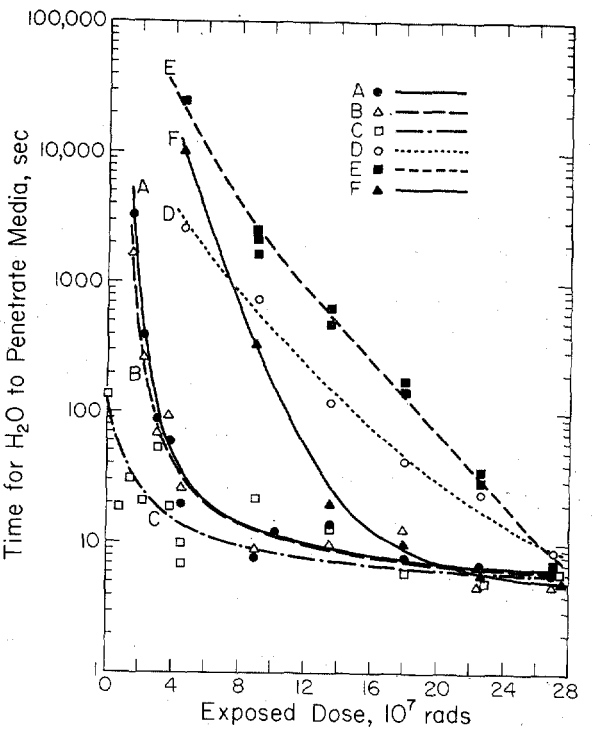

FIGURE 14. HEPA FILTER MEDIA WATER REPELLENCY VS EXPOSED GAMMA DOSE

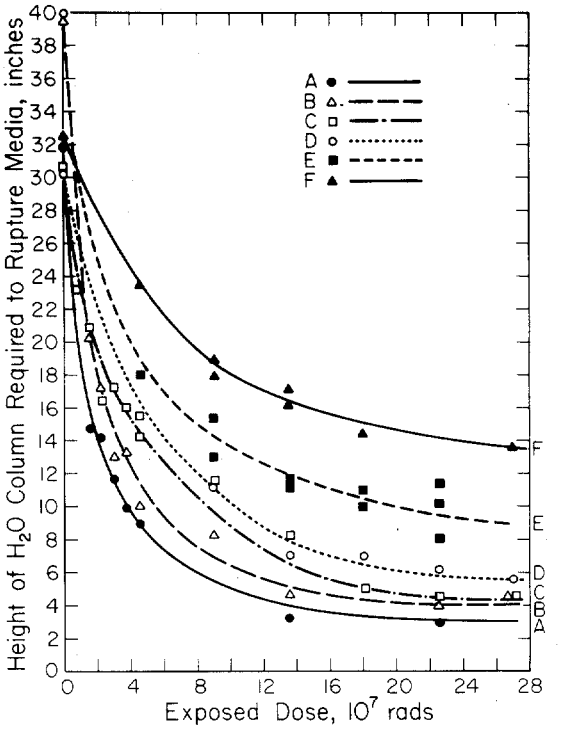

FIGURE 15. HEPA FILTER MEDIA WET STRENGTH VS EXPOSED GAMMA DOSE

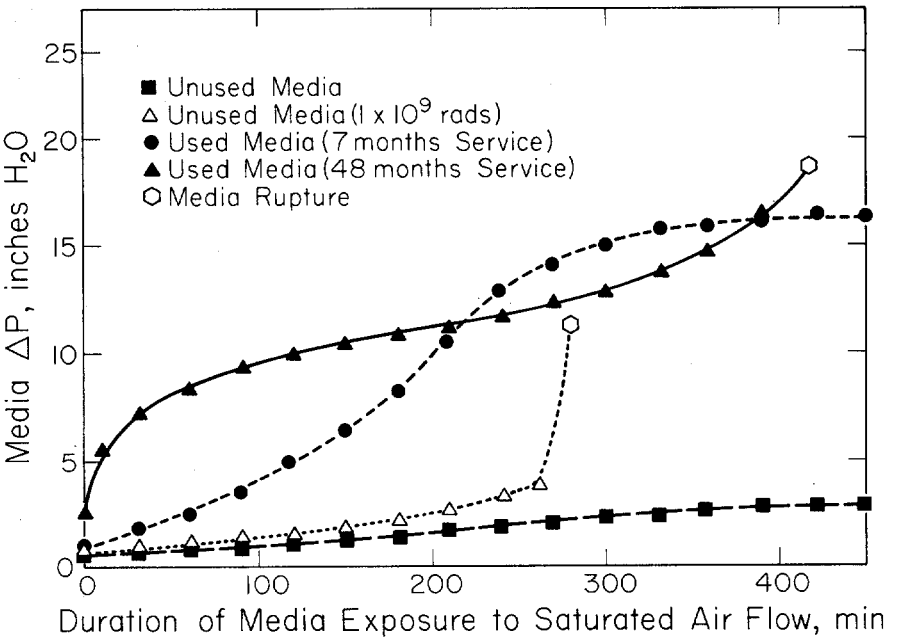

FIGURE 16. EXPOSURE OF SRP HEPA FILTER MEDIA TO SATURATED AIR FLOW

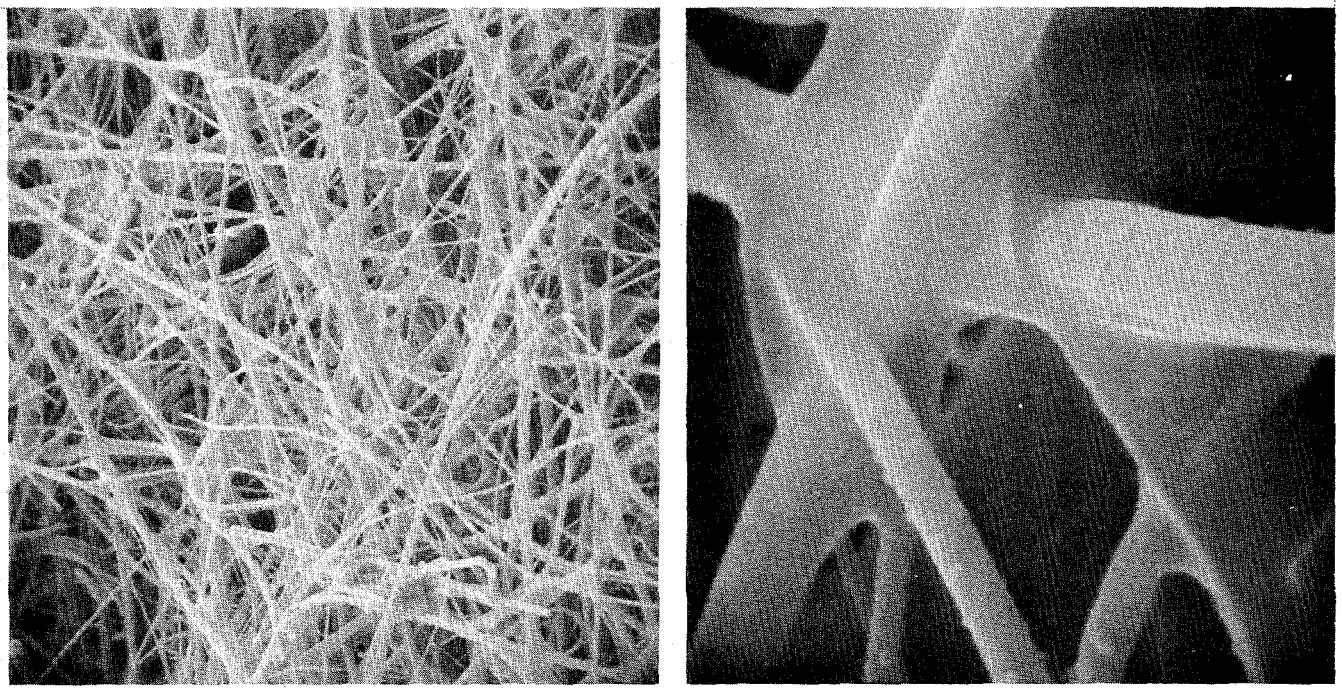

590X Unirradiated 11700X

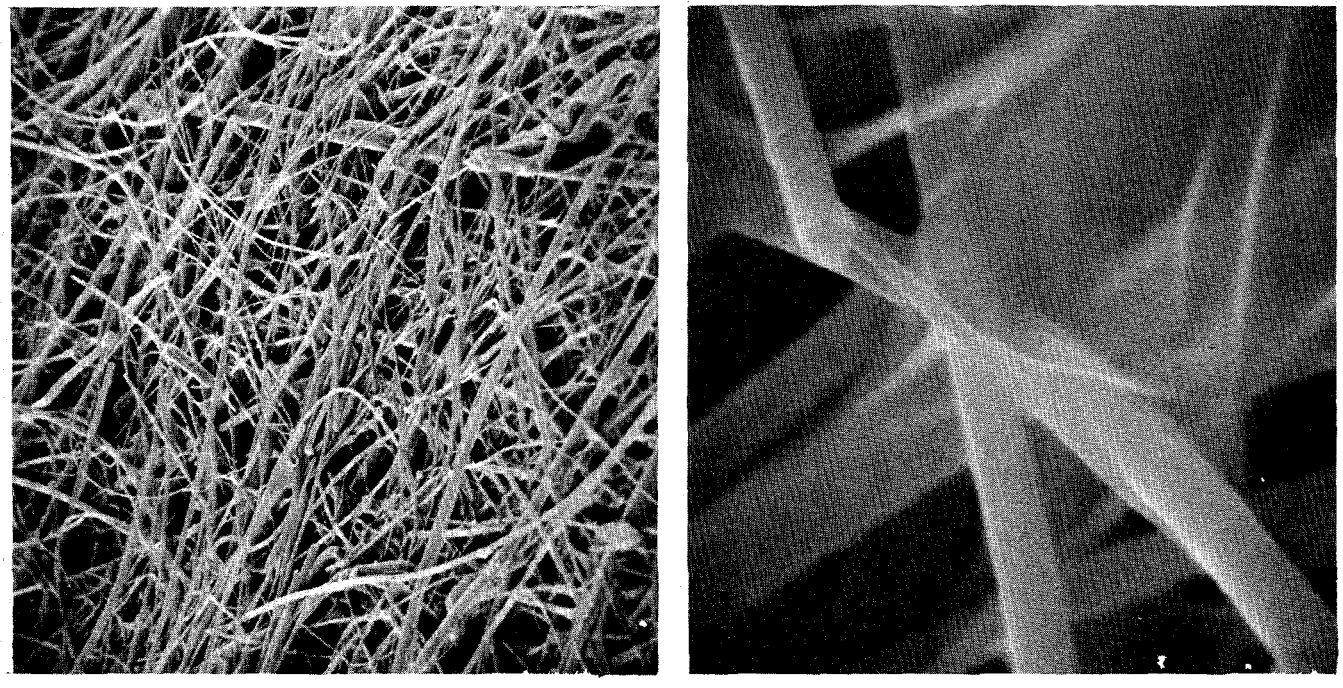

620X Irradiated 12300X

FIGURE 17. SCANNING ELECTRON MICROSCOPE EXAMINATION OF IRRADIATED HEPA FILTER MEDIA

250X

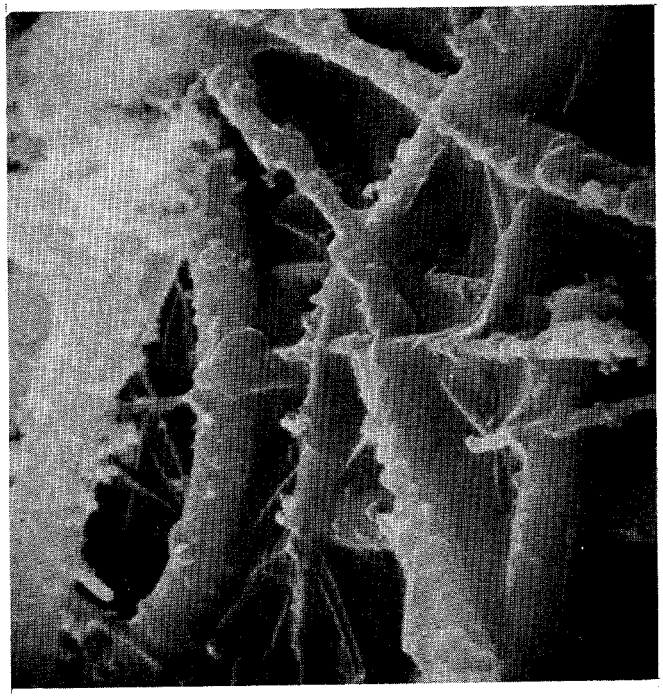

Upstream Face 6200X

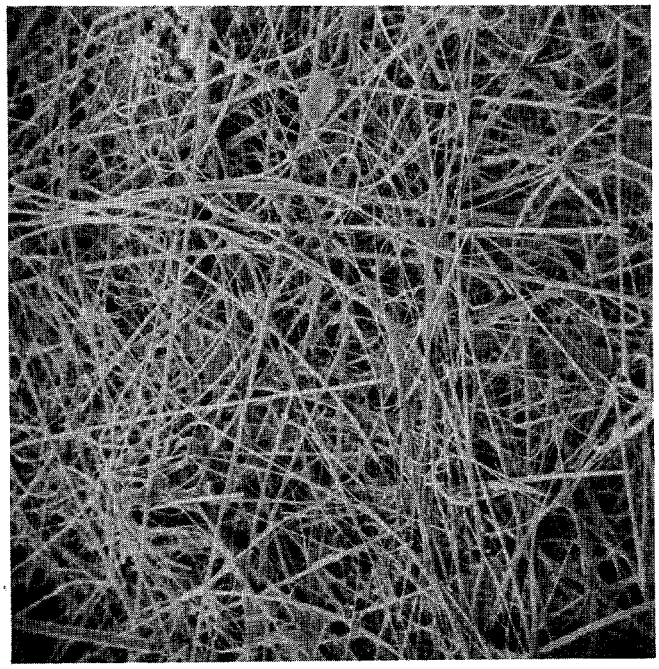

235X

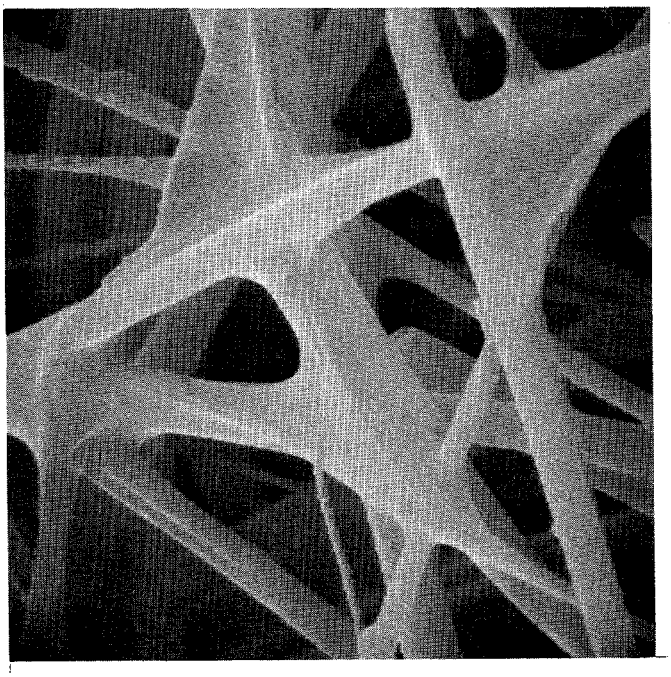

Downstream Face 5900X

FIGURE 18. SCANNING ELECTRON MICROSCOPE EXAMINATION OF USED HEPA FILTER MEDIA

DISCUSSION

HUTTEN: I have three questions. The first two concern your sample radiation container. You stated that the sample was purged continuously with dry air and the temperature monitored?

JONES: Right.

HUTTEN: Would you tell us how the temperature was monitored and what temperatures you observed?

JONES: We monitored the air temperature inside the container. The reason it was purged with clean, dry air was to prevent build-up of NO_2, ozone, and gases from radiolysis of air, as well as gases from the decomposition of the materials. The temperature of the air ran approximately 70 to 80° C, because this is aproximately the temperature of the water inside that circle of cobalt slugs. The temperatures of the materials are estimated as we didn't have thermocouples imbedded in them.

HUTTEN: My third question conerns Table 4. The properties of media E are not included in that table. Could you explain why, and are these properties available?

JONES: At the time the evaluations were made, we didn't include that material. It is the material we use in the SRP confinement system and is similar to material D, with somewhat less waterproofing agent.

PERFORMANCE OF ABSOLUTE FILTERS AT TEMPERATURES FROM AMBIENT TO 1000°F

Melvin W. First
Harvard School of Public Health
665 Huntington Avenue
Boston, Massachusetts 02115

Abstract

Sodium chloride aerosols have been used to test the penetration of filter papers and commercially fabricated absolute filters over the temperature range 150 - 1000°F. Although filtration theory indicates that penetration should decrease at elevated temperatures, this effect was not observed in practice. In some cases, obvious structural failures were observed after high temperature exposure, but even filters which appeared to be undamaged after heat exposure may have suffered some internal degradation that accounted for the failure to show a decrease in penetration. The principal structural failure occurred to aluminum corregated separators which lost their stiffness above 800°F. As the softened separators sagged, they permitted the filter pack to part from the top seal. Initial results indicate that sodium chloride aerosols can be used to evaluate the efficiency of filters at elevated temperatures.

I. Introduction

Heat tolerance and fire resistance of standard and specially constructed absolute filters have been greatly improved by the continuing program of the Division of Operational Safety, AEC. Although these filters are intended to be fully functional up to the limit of their structural integrity, little information is available regarding the effects of high temperature on absolute filter efficiency and air flow capacity. Theoretical analyses of the probable effects of elevated temperature provide a guide to performance only when there are no internal changes within the filter membrane or to the gross filter structures which seal the membrane to the filter casing. As many detrimental changes at high temperature may be reversible when the filter returns to ambient temperature, DOP testing before and after heating, though widely used for assessing heat and flame damage (1), is not a fully reliable guide to filter behavior at high temperature. Therefore, a simple standard method for measuring filter efficiency and airflow capacity at elevated temperature is required and the results of such measurements are needed to assign correct filter efficiencies and capacities to filters under stress when estimating the effectiveness of engineered safeguards.

The British standard test for high efficiency filters (BS3928) uses a sodium chloride aerosol generated by atomization and drying

of a salt solution of appropriate strength and evaluates filter penetration with a sodium flame penetrometer. Sodium chloride particles are excellent for temperatures up to 1000°F, but the British test method has some serious drawbacks (2) which include (a) particle size substantially different from 0.3 μm, which is considered optimum for high efficiency filter testing, (b) low salt concentrations in the test aerosol and (c) insufficient sensitivity of the sodium flame penetrometer to cope with the very low salt concentrations that penetrate high efficiency filters when the upstream concentration is low. Generation of high concentrations of small particles by atomization and drying of salt solutions has the added disadvantage of introducing large amounts of water vapor into the system and requiring long drying tunnels for droplet evaporation.

At the 11th AEC Air Cleaning Conference (3), Dyment suggested vaporizing salt in an oxyacetylene flame as an alternate method of generating a sodium chloride aerosol of small size and high concentration without the use of water, and he and his collegues subsequently developed this technique further (4).

A number of studies have been conducted to assess the equivalence of salt and DOP aerosols generated by a number of established methods for filter testing (5,6). Except for resin-impregnated wool filters, which depend upon electrostatic charge effects that are destroyed by deposition of oily DOP, test results are equivalent though not necessarily equal over the range of flow rates customarily used with high efficiency filters. Predictable penetration differences occur when using monodisperse vs. polydisperse aerosol particles of the same mean size and when using polydisperse particles having slightly different mean size or size distributions. Nevertheless, many years of successful experience has indicated that anyone of several systems of aerosols and penetrometers can be relied upon to rate high efficiency filters properly even though certain of these standard tests may be less convenient or more costly than others. This experience suggests that the method used for testing absolute filters at elevated temperature need not give precisely the same penetration numbers as the standard USAEC 0.3 μm DOP test aerosol to be useful. The use of a high temperature test aerosol plus a standard DOP test aerosol under identical flow conditions at ambient temperatures is an aid in interpreting high temperature test results and provides the greatest amount of information about overall filter efficiency. Therefore, both tests should be used simultaneously within the appropriate temperature range.

II. Vapor Pressure of Sodium Chloride at Elevated Temperatures

Although there have been references to a rather modest limit to the elevated temperature usefulness of sodium chloride aerosols (e.g., 572°F (7,8)), (presumably because the amount of sodium vapor in the filtered air adds significantly to the penetration value when tested by the sodium flame penetrometer) there does not appear to be a sound basis for this belief.

In one instance (8), calculated vapor pressures for temperatures below 1000°F were based on extrapolated values from vapor pressure data for liquid sodium chloride (M.P. 1472°F) without taking into account that a change in slope of the vapor pressure curve takes place when the substance undergoes a change of state and, hence, a change in the heat of vaporization. In addition, over wide temperature ranges, plots of the log of vapor pressure vs. the reciprocal of the absolute temperature are somewhat curved because the heat of vaporization varies with the temperature (9). Therefore, as it is not possible to calculate the vapor pressure of solid sodium chloride with reliability from available data, experimental determinations of sodium chloride evaporation were made over a range of temperatures up to 1000°F. The salt was exposed to an even temperature in a muffle furnace over a period of several days and weighed daily after cooling in a dessicator. To prevent saturation of the furnace atmosphere, a constant flow of dry nitrogen was maintained through the chamber throughout each experiment. After an initial weight loss of water vapor (24-48 hours), no further weight reduction was noted. A typical result was as follows: Fifteen grams of sodium chloride did not lose a measurable amount of weight (after an initial moisture loss) even after four days in a muffle furnace at 1000°F. It may be concluded, therefore, that the vaporization of sodium chloride at temperatures below 1000°F does not represent a serious error in the determination of filter penetration when using a salt aerosol; especially since the error, if any, is on the conservative side.

III. Aerosol Generator and Test Tunnel

Figure 1 is a photograph of the completed experimental assembly for conducting high temperature filter efficiency and pressure drop tests on absolute filters having nominal cross-sectional dimensions of 8"x8". Starting from the left of the photo, it consists of an aerosol generator, a test tunnel, dual flame photometers for simultaneously measuring aerosol concentrations up and downstream of the test filter, an exhauster with airflow meter and flow regulating device, and multiple pressure taps and thermocouple leads at appropriate locations. Sampling points have been provided at several locations to monitor size distribution and cross-sectional concentration uniformity. This is illustrated by the electrostatic precipitator, located at point 8, used to obtain a sample for examination under the electron microscope for sizing. The test aerosol is prepared by vaporizing salt in an oxygen-acetylene flame with the use of a Model C, Wall Colmonoy* spray welder unit. This is an apparatus used for applying powdered metal alloys to metal surfaces for building up the surface. Salt is prepared by a method described by Dyment (3) in which a mixture of salt plus 25% by weight colloidal graphite** is ground in a mortar and sieved through a 200 mesh screen, dried at 110°C, reground and re-dried. The objective in the preparation of the salt mixture is to produce finely divided salt particles coated on the surface with finely divided graphite to make them free-

* 19345 John R. St., Detroit, Michigan 48203

** Joseph Dickson Crucible Company, Jersey City, N. J.

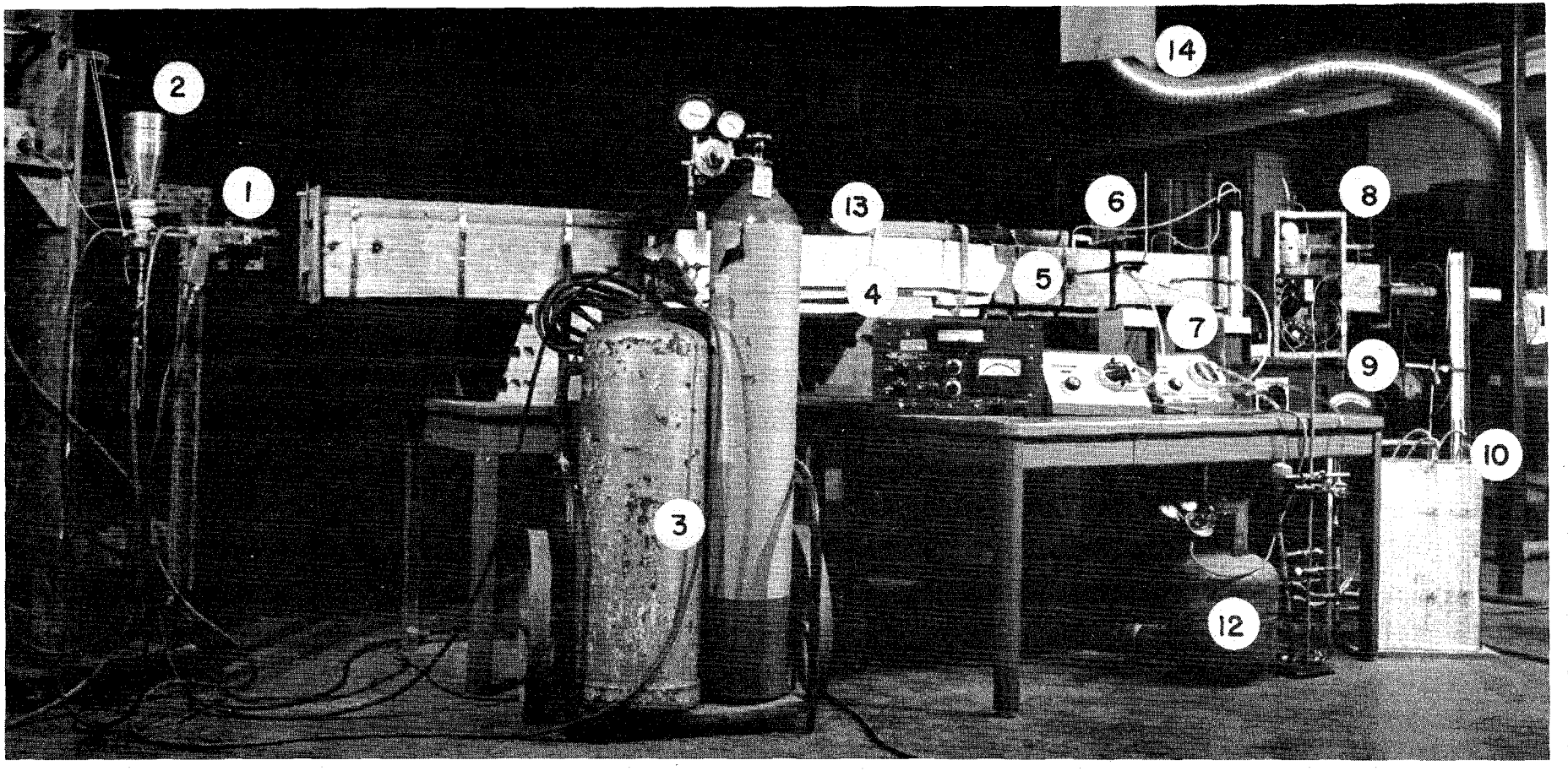

1. METALIZING GUN AEROSOL GENERATOR
2. FEED HOPPER FOR GENERATOR
3. OXYGEN AND ACETYLENE FOR GENERATOR
4. DIFFERENTIAL PHOTOMETER
5. SAMPLE PROBES
6. FILTER
7. FLAME PHOTOMETERS WITH PERISTALTIC PUMPS
8. ELECTROSTATIC PRECIPITATOR
9. PYROMETER (FILTER AND FLOW METER)
10. MANOMETERS FOR FILTER FLOW AND FLAME PHOTOMETER FLOW MEASUREMENT
11. BLOWER
12. PROPANE FOR FLAME PHOTOMETERS
13. 7" X 7" INSULATED TUNNEL WITH FLOW MIXERS AND STRAIGHTENERS
14. EXHAUST AEROSOL TO WASTE

FIGURE 1. SODIUM CHLORIDE AEROSOL TEST APPARATUS.

flowing in the powder feeding system and non-caking during storage and handling.

The spraywelder gun is fed with 15 lpm acetylene, 12 lpm oxygen, plus 33 lpm dry compressed air to fluidize the powder and convey it to the gun. The graphite coating is oxidized to CO_2 in the flame and the salt is totally vaporized. After leaving the intense heat of the oxy-acetylene flame, salt vapor condenses into submicron sized cubic particles as shown in Figure 2, an electron micrograph of typical aerosol particles collected by electrostatic precipitation. If the hot gases are not cooled promptly, extensive agglomeration occurs, as shown in Figure 3. The individual particles in Figure 3 are larger than in Figure 2 as vapor continues to condense on small particles while the temperature is elevated and the more vigorous Brownian motion at higher temperature encourages collisions between particles.

After the two flame penetrometers have been adjusted to read the same when sampling at the same location in the duct, the units may be used to measure salt concentration up-and downstream of a test filter. The sampling and measurement systems consist of a peristaltic pump to extract a sample from the test duct at a constant gas flow rate and pump it into a flame unit without serious loss of particles in the pump. The detection system consists of a laboratory burner fueled by propane (item 12, Figure 1), a Baird Atomic, Inc.* flame penetrometer chamber, an RCA 1P22 detector tube, and an Eldorado Electronics**Model 210 dual channel differential penetrometer. An aerosol concentration-meter response calibration curve for the sodium aerosol determination system is shown in Figure 4. The lower detectable limit for the apparatus is 0.1 mg/M^3, making it possible to evaluate filter efficiency to 1 part in 2,000.

The size distribution of the salt aerosol particles shown in Figure 2 has been determined by measuring individual particles with a scale. Figure 5 has the size-by-count distribution curve for the particles shown in Figure 2. The count median diameter is 0.064 μm and the geometric standard deviation is 1.7. By calculation, the mass median diameter of the size distribution is 0.14 μm and the derived size-by-weight distribution curve is also shown on Figure 5.

IV. Test Results

A. Heat Shrunk Quartz Fiber Paper.

A number of 6 x 6 inch sheets of an experimental high temperature filter paper weremade available for test through the courtesy of W. L. Anderson, Naval Research Laboratory†. A separate sheet was used for each test at a different temperature to avoid changes in penetration caused by a buildup of salt in the filter matrix. The results of seven test series, each at a different temperature are summarized in Table 1. The mass gas flow rate was kept approximately

* 125 Middlesex Turnpike, Bedford, Massachusetts

** 2821 Tenth Street, Berkeley, California

† Current affiliation, Naval Weapons Laboratory

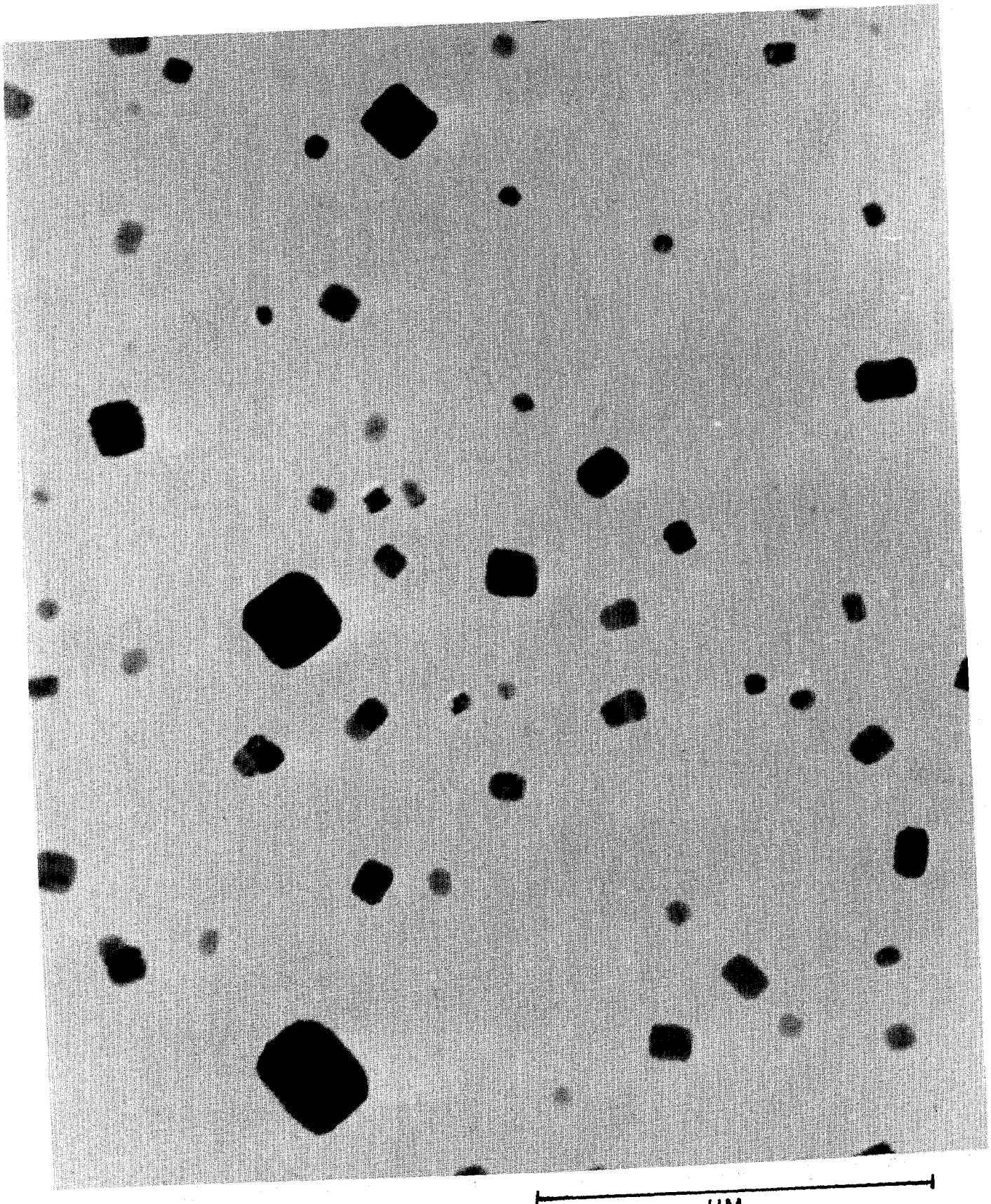

FIGURE 2. SODIUM CHLORIDE AEROSOL

FIGURE 3. AGGLOMERATED SODIUM CHLORIDE AEROSOL.

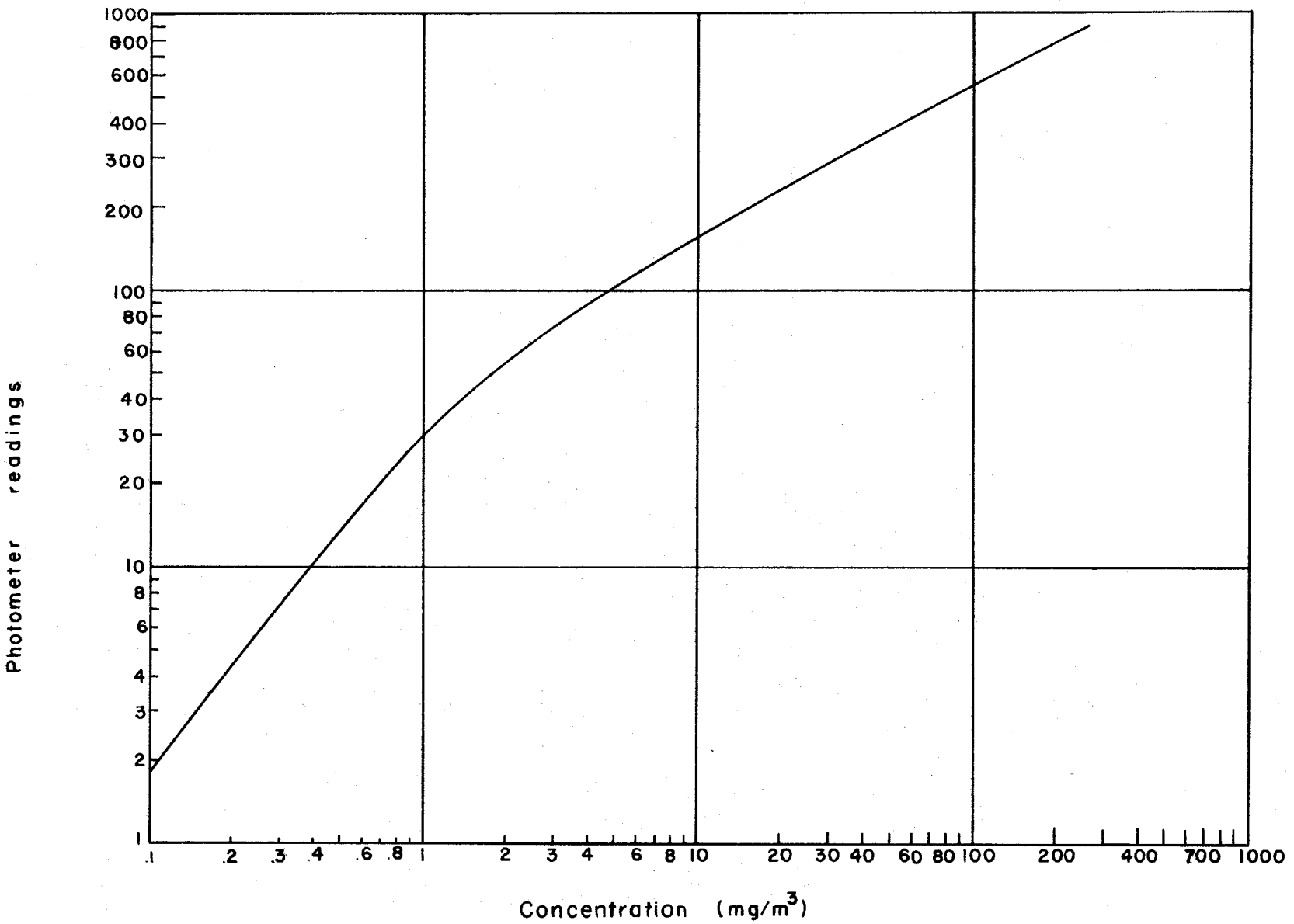

FIGURE 4. SODIUM FLAME PHOTOMETER CALIBRATION.

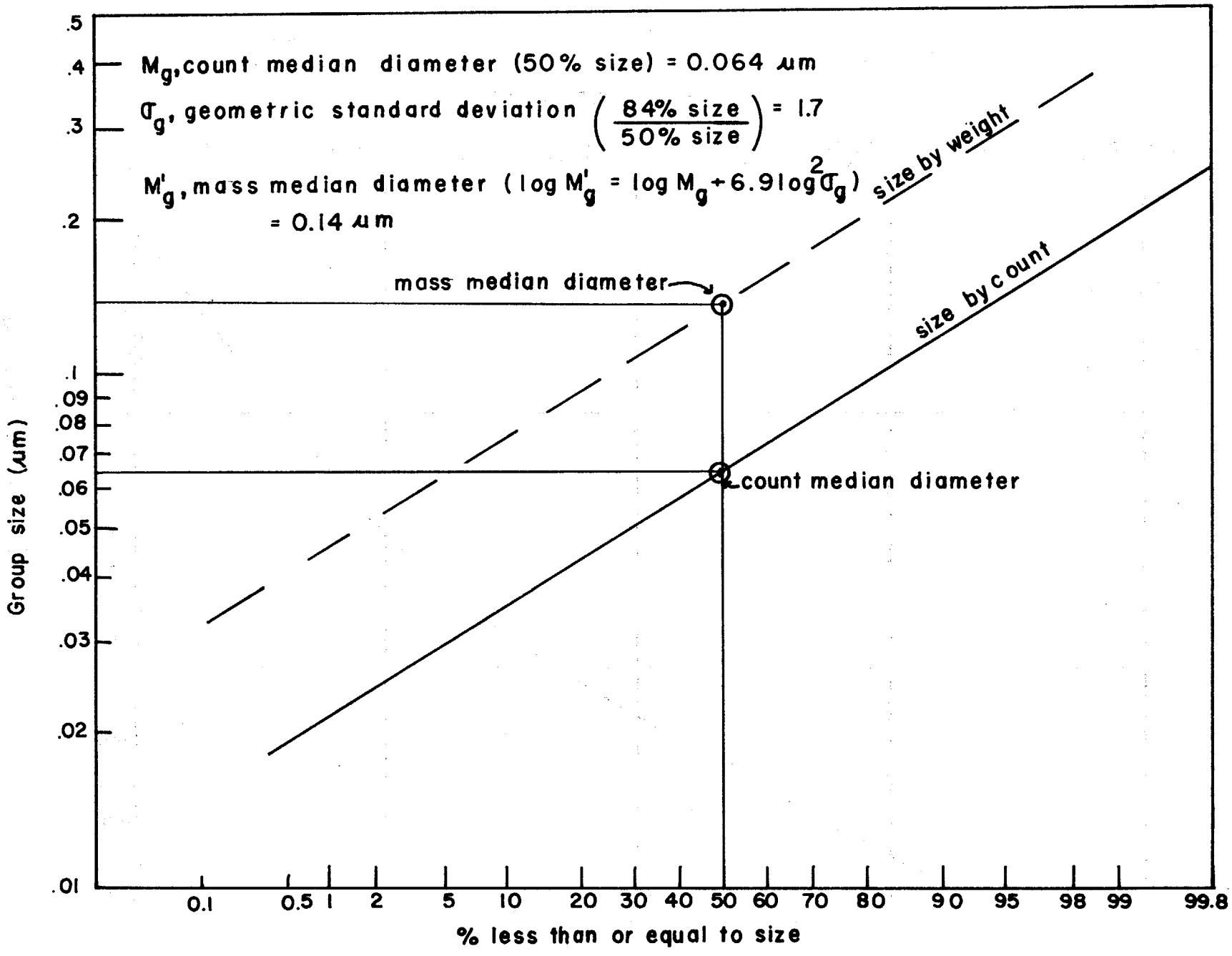

FIGURE 5. SIZE DISTRIBUTION OF PARTICLES SHOWN IN FIG. 2

TABLE 1

Heat Shrunk Quartz Fiber Paper

Paper No.	DOP Pen.[1]--% Before	After	Temp. °F	Face Vel.[2] at temp. fpm	No. Salt Tests	Salt Pen.--% Av.	Range[3]	Filter resistance at temp. in.w.g. Start	End	Duration of test (min)	Salt conc'n mg/M^3 at temp.
1	--	--	225	33.7	4	.043	.039-.054	3.7	13.3	4.5	45.6
2	.72	.62	380	41.7	12	.074	.042-.137	6.7	16.8	10.5	26.1
3	.57	.47	580	49.4	15	.055	.023-.100	8.4	15.0	14.0	26.6
4	.50	.42	660	53.2	12	.078	.050-.115	10.0	15.4	11.0	13.2
5	--	--	780	55.6	11	.048	.025-.058	8.6	14.2	26.0	11.9
6	--	--	840	59.5	15	.063	.036-.079	13.0	15.1	24.0	11.1
7	--	--	950	62.4	10	.032	.020-.050	14.8	16.8	18.0	15.5

Notes:

1 With NRL cold DOP generator and ATI Penetrometer

2 Mass gas flow approximately constant throughout the entire test program

3 Variations in penetration were random throughout each series of tests

constant through the test series. As a consequence, filtration face velocity increased with increasing temperature and salt concentration decreased in terms of weight per standard volume of gas. The results (Table 1) are reported in terms of actual volumetric flow at the indicated temperature.

Three papers were tested with cold DOP at ambient temperature before and after exposure to heat and the sodium chloride aerosol. Although the papers were believed to be identical, the clean DOP efficiency varied significantly from piece to piece. Following heat and sodium chloride exposure, each of the papers showed a decreased in DOP penetration of approximately 0.10 per cent. Average NaCl penetration of the seven papers ranged from .032 to .078% with no consistent trend with respect to test temperature. Individual readings of sodium chloride efficiency varied as much as ± 50% about the mean during each test series on an identical paper. It is believed that this resulted from difficulties associated with achieving good aerosol mixing in the inlet duct at the very low flow velociites that must be used when testing a single sheet of paper.

The paper showed no effect of heat stress on physical properties or penetration even at the highest temperature. It is apparent from the test results that penetration of DOP is far higher than for absolute filter papers prepared from glass fibers. Salt penetration is approximately one order of magnitude less in spite of the fact that the salt particles have approximately 1/4 mass median diameter. The reasons for this difference were not investigated. The explanation may be destruction of electrostatic charges on the quartz fibers by DOP or more effective removal of the smaller particles by diffusional separating forces.

B. Commercial 8 x 8 x 12 inch AEC Filters

Two types of high temperature resistant pleated filters were tested: one type was composed of glass fiber paper, aluminum separators, stainless steel frame, and ceramic and glass fiber edge sealers*; the other type contained identical components except that the aluminum separators were eliminated and the filter paper was corrugated in a way which kept the folds apart**. Both types were equipped with glass paper end gaskets. The manufacturer's standard test at 100 cfm flow rate for two of each type showed the following results:

		Resistance	Penetration
Filters with Separators	1	.90 in.w.g.	.018%
	2	.94 in.w.g.	.010%
Filters w/o Separators	1	.74 in.w.g.	.020%
	2	.78 in.w.g.	.020%

* Flanders Filters, Inc., Stock No. 7C31-G

**Flanders Filters, Inc., Stock No. 7031-G

Each filter was tested with sodium chloride aerosol at temperatures ranging up to 1000°F. The results are summarized in Table 2. For each of the four filters, there is a marked increase in penetration at temperatures of 800-1000°F. Penetration decreases when the filter is cooled and in some cases returns to low pre-heat values whereas, in others, penetration is permanently increased. This behavior indicates that structural changes occur at elevated temperature that adversely affect filter efficiency. Some of these are temporary and the strucutre returns to normal when the filter is cooled; others are permanent and become worse on prolonged exposure to high temperature. Figure 6 shows the type of damage that takes place gradually on prolonged (several hours) exposure to 1000°F. The metal casing expands, warps, and thereby puts a strain on the seams of the casing which causes them to open. The 8 x 8 x 12-inch filter is probably prone to this type of damage because depth is 1.5 times the face dimensions. For the most widely used size, 24 x 24 x 12-inch, the depth is only 0.5 times the face dimensions and longitudinal wracking is less likely to produce deflections great enough to split the casing seams. Nevertheless, temporary bulging of the casing,to create leaks at elevated temperature that disappear on cooling, cannot be ruled out.

A smaller filter size (8 x 8 x 6-inch) showed a small, but perhaps significant, increase in penetration at 800-1000°F, as shown in Table 3 which summarizes tests on filters identical with those discussed above except that the filter depth was 6 inches instead of 12 inches and the gasket seal was made in a grease-filled slot instead of a compressible face gasket. Nevertheless, on prolonged testing at 1000°F, this casing, too, is subject to expansion, warping, wracking, and permanent damage, as shown in Figure 7. The nail that has been inserted into the opening is for illustrative and comparison purposes; it is not forcing or holding the metal layers apart.

Other types of physical damage which occur under heat are illustrated in Figures 8 and 9. Figure 8 shows the face of a filter constructed with aluminum separators and glass packing edge seals. The aluminum separators have softened and permitted the filter pack to slump away from the top of the casing, opening a wide gap. Figure 9a shows the face of a new separator-less filter and Figure 9b shows the same filter after heating to 1000°F. The filter paper has shrunk and the pack has lost its dimensional stability. These phenomena are not unique to the several types of filters that have been used for illustration. All filters tested, from several manufacturers, exhibit similar damage under identical exposure conditions.

C. Tests of 24 x 24 x 12 inch Filters

The fire instrusion-high temperature test facility at Lawrence Livermore Laboratory(1) (in somewhat modified form) was used to test 1,000 cfm filters at high temperatures with the same appartus used to perform the laboratory studies described earlier. Figure 10 shows the equipment in operating condition. Penetration data at ambient temperature and at elevated temperatures duplicated those

TABLE 2

Penetration Tests at Various Temperatures
Flow Rate--100 cfm at temp.

Test Temperature °F	7C31-G Filters		7031-G Filters	
	No. 1	No. 2	No. 1	No. 2
70	.012*	.020*	.020*	.010*
70	--	.062	.094	.081
200	.038	.082	.097	.065
400	.032	.071	.10	.062
600	.033	.092	.10	.058
800	.046	.11	.16	.063
1000	.053	1.2	.50	.17
800	.074	.11	.26	.082
600	.040	.076	.21	.082
400	.029	.073	.21	.077
200	.036	.082	.22	.077
70	.036	.059	.16	.080
70	.050*	.060*	.020*	.010*

* Cold DOP Test

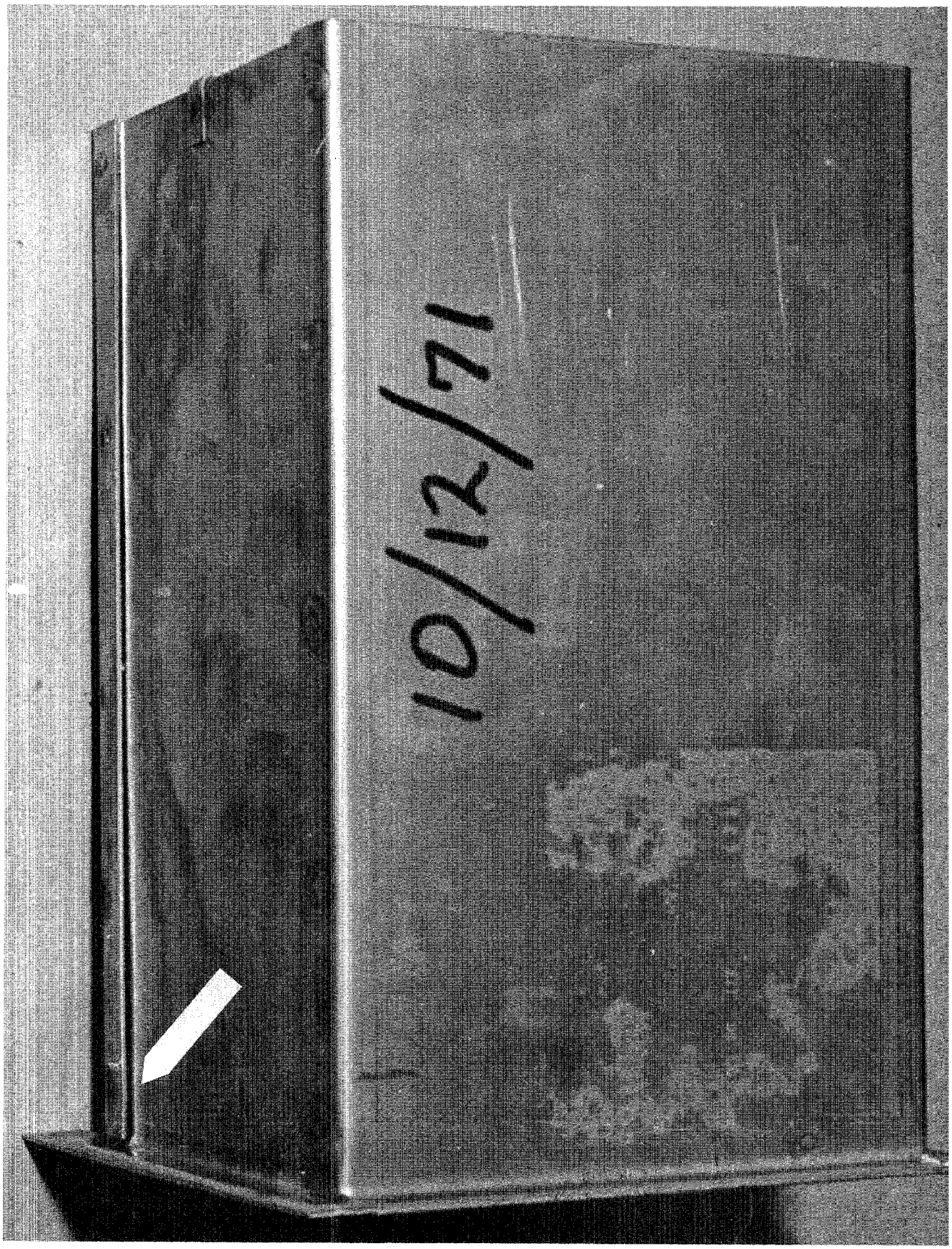

FIGURE 6. CASING FAILURE OF 8"X 8" X 12" FILTER.

TABLE 3

EFFICIENCY TESTS-SALT AEROSOL
(8"x8"x6" Absolute Filters)

Filter	Flow Rate cfm at STP	Temp. °F	Penetration Salt wt. %	Penetration DOP %
1-Separatorless	50	70	.037	.026
		200	.028	
		400	.022	
		600	.032	
		800	.049	
		1000	.062	
2-Separators	50	70	-	.017
		200	.052	
		400	.052	
		600	.064	
		800	.076	
		1000	.074	

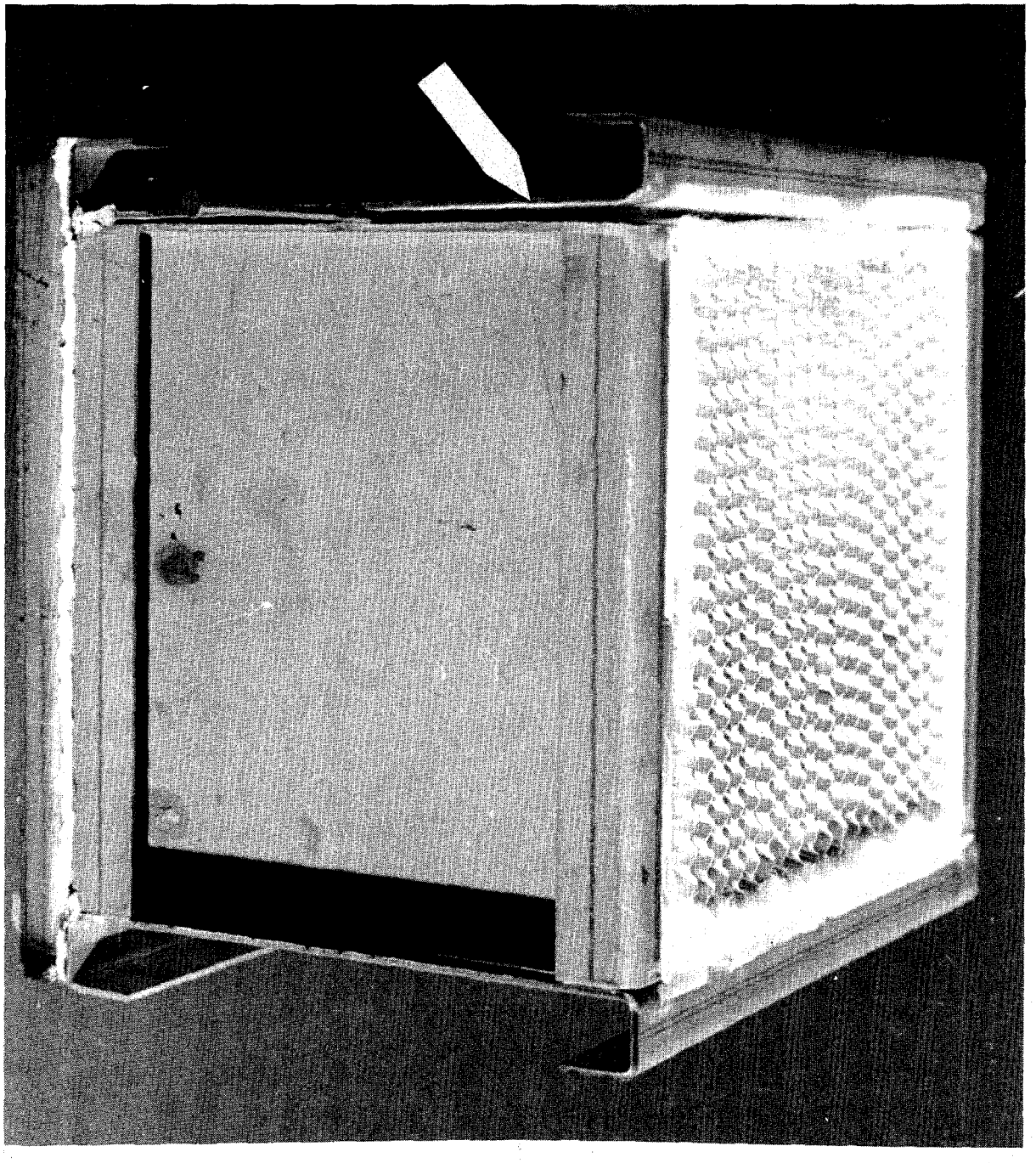

FIGURE 7. CASING FAILURE OF 8" X 8" X 6" FILTER.

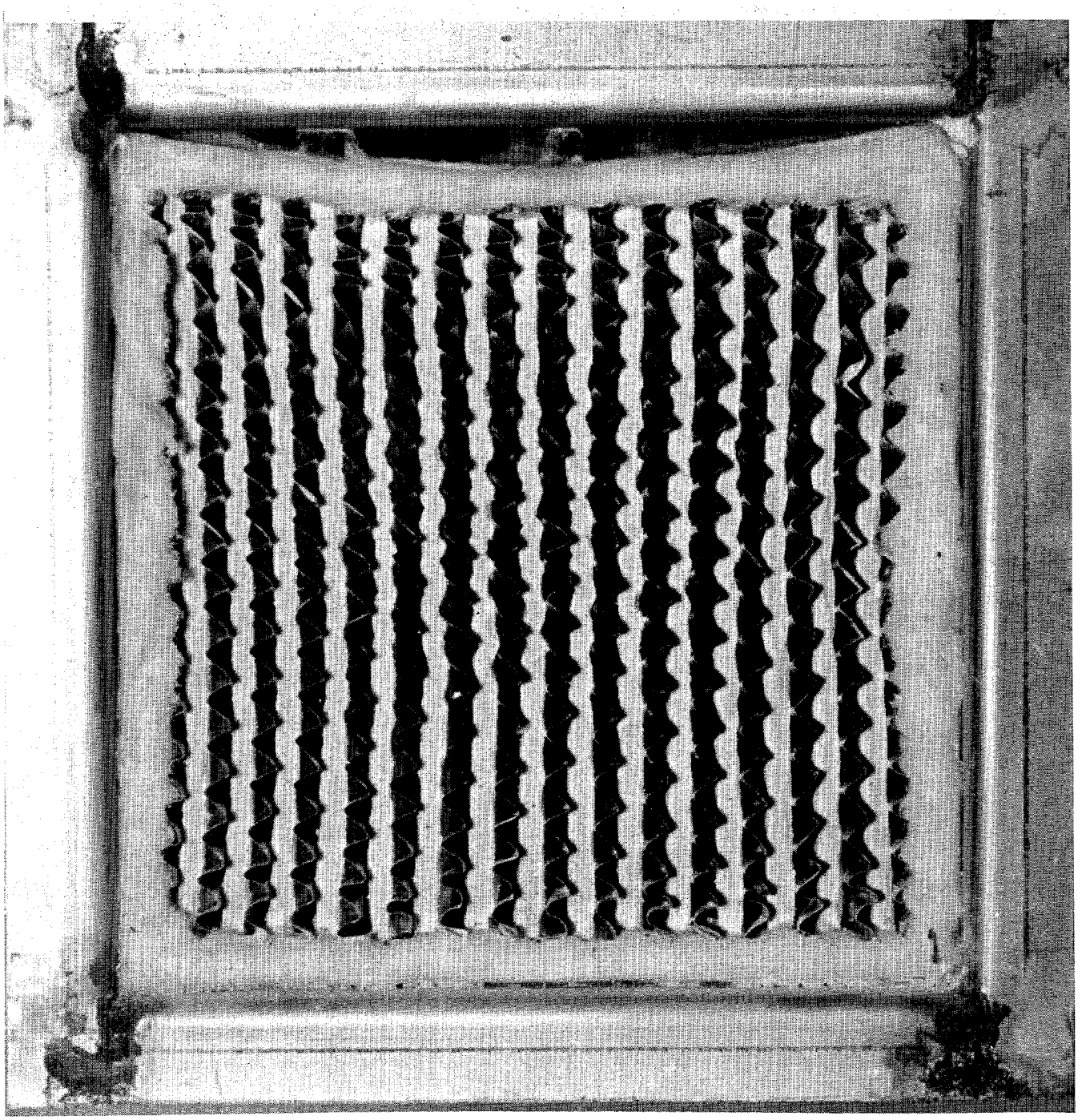

FIGURE 8. FILTER FAILURE FROM SOFTENING OF ALUMINUM SEPARATORS.

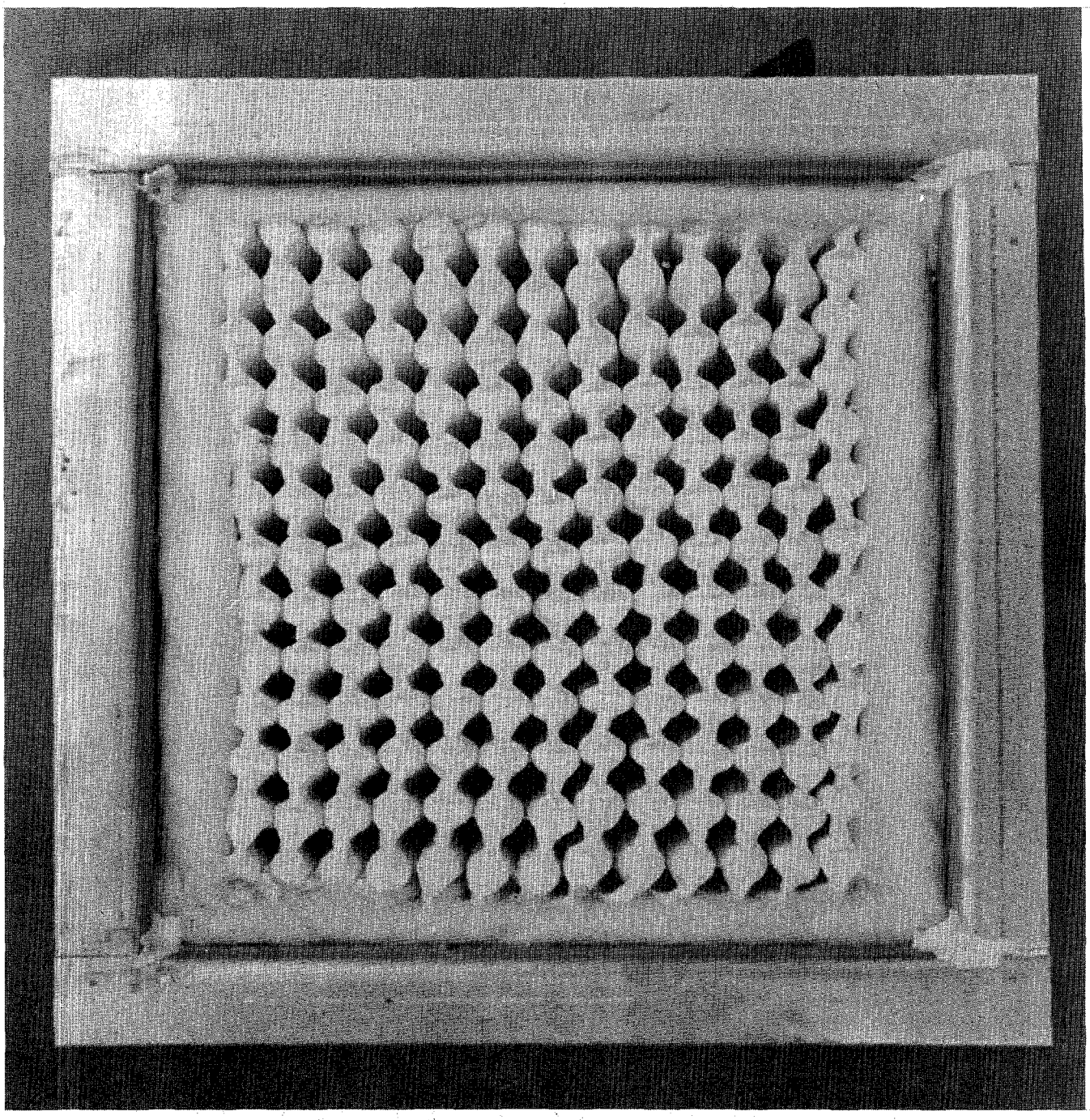

FIGURE 9A. SEPARATOR-LESS FILTER BEFORE HEAT STRESS.

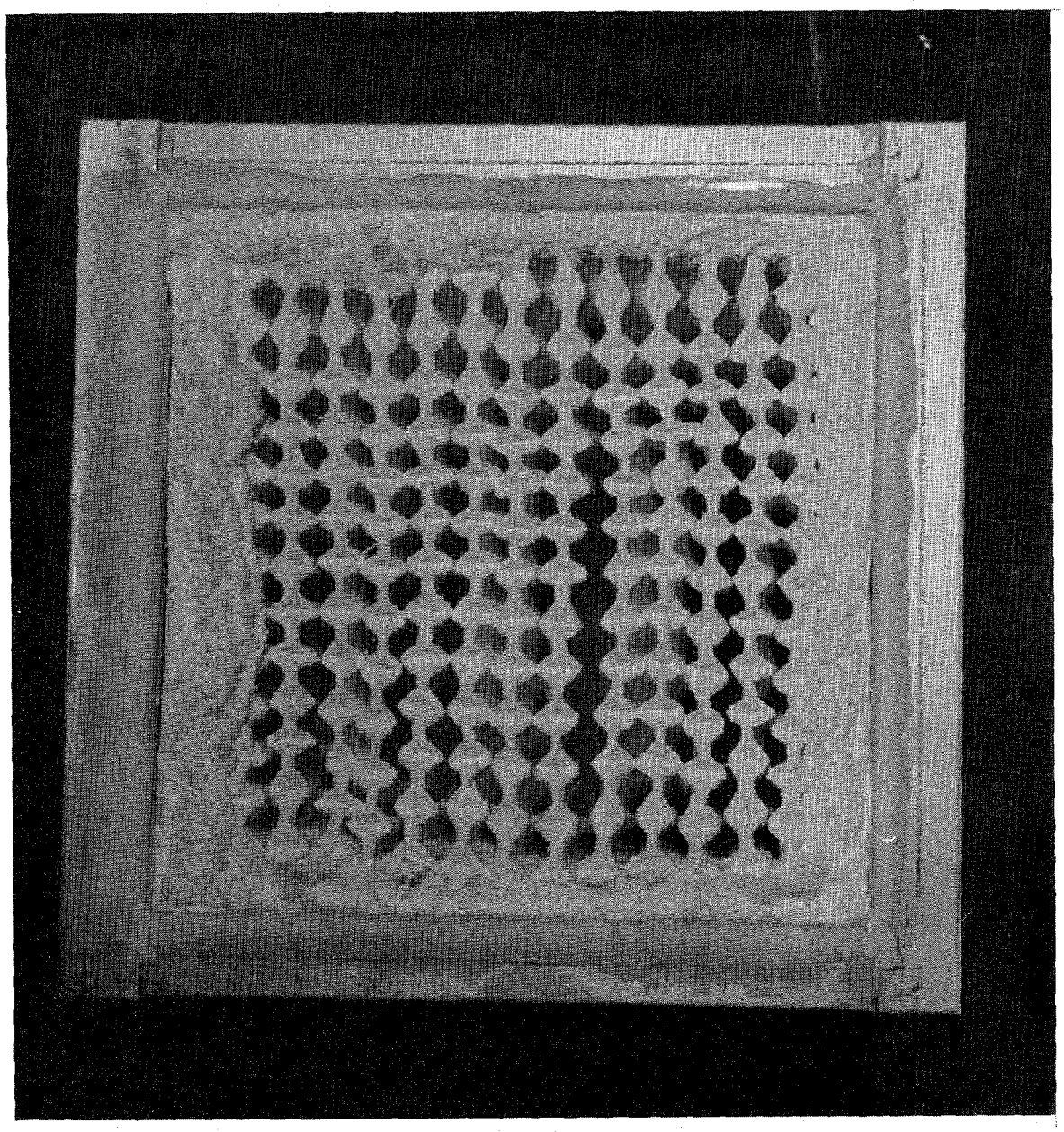

FIGURE 9B. SEPARATOR-LESS FILTER AFTER HEAT STRESS.

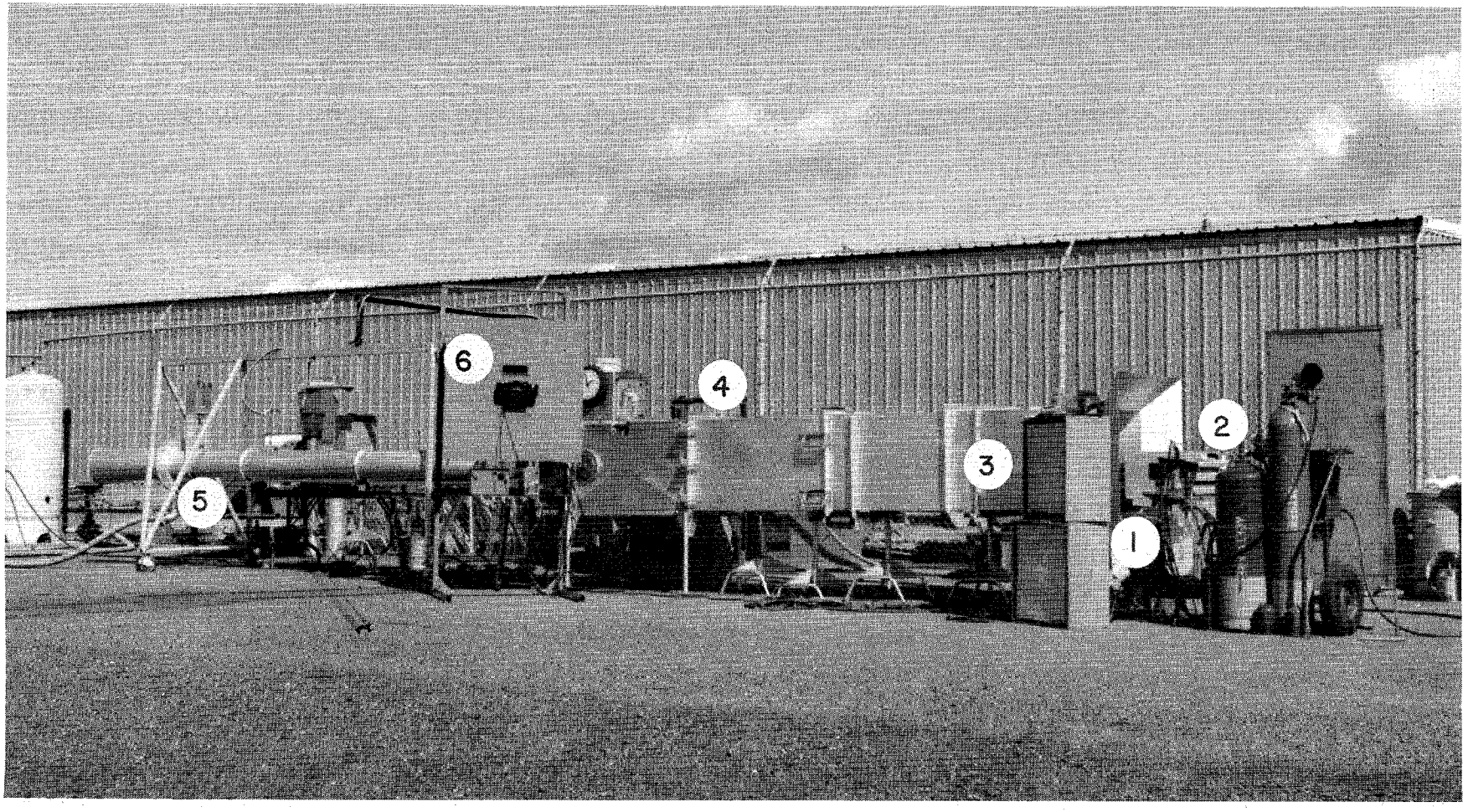

1. SODIUM AEROSOL GENERATOR
2. GAS HEATERS
3. MIXING TUNNEL
4. FILTER STATION
5. AIR FLOW EDUCTOR
6. DATA RECORDER

FIGURE 10. FULL SCALE TEST APPARATUS AT LAWRENCE LIVERMORE LAB. (PHOTO. COURTESY OF LAWRENCE LIVERMORE LAB.)

found in the laboratory and indicated that laboratory results on small filters provide a guide to the performance of full scale filters. Similar types of heat damage occur to large filters as to small, as illustrated in Figures 11a and 11b, which show the front and rear of a 24 x 24 x 12 inch filter constructed from glass filter paper, aluminum separators, metal casing, and fiber packed edge seals. These photos may be compared with the small filter illustrated in Figure 8 which shows identical failure.

V. Discussion and Conclusions

One of the major questions which stimulated interest in a high temperature test program--namely, whether a filter which tested satisfactorily after cooling gave the same high filtration performance at elevated temperature--appears to have been answered in the negative. Many individual filters withstand heat stress well for brief periods (whereas others of identical construction fail, for reasons which are not yet clear) but all degrade under prolonged heat stress and most fail structurally. Although gross structural failures are readily apparent without the use of sophisticated test procedures, the sodium chloride aerosol test is capable of detecting high temperature filter failures which disappear on cooling or are of such nature that they are hidden from view.

Tests of flat sheets of heat shrunk quartz paper indicate that the paper does not degrade under heat stress although the variability in the test results caused by very low gas flow rates and poor aerosol mixing may have obscured small changes. Although similar tests should be conducted on widely used grades of glass fiber paper on the basis of the media shrinkage exhibited by the filter shown in Figure 8b, the tests reported here suggest that structural failure of the filter cartridge, rather than the filter paper, is responsible for increased penetration under heat stress.

It may be concluded from the information already available, that new materials and new construction techniques are required for filters which must give continuous high efficiency collection under prolonged heat stress.

References

1. Murrow, Jack L., "Effect of Fire Intrusion and Heat on HEPA Filter Units", Proceedings of the 9th AEC Air Cleaning Conference, Boston, Massachusetts (13-16 September, 1966).

2. Dorman, R. G., and Webb, I. J., "An Improved Sodium Flame Test for Air-Conditioning Filters of Very High Efficiency", Chemical Defense Establishment, Porton Down, Wiltshire, England (29 March 1971).

3. Dyment, J., "Present Status of the Design and Testing of Radioactive Filtration Installations and Associated Aerosol Research" Proceedings of the 11th AEC Air Cleaning Conference, Richland, Washington (31 August-3 September, 1970).

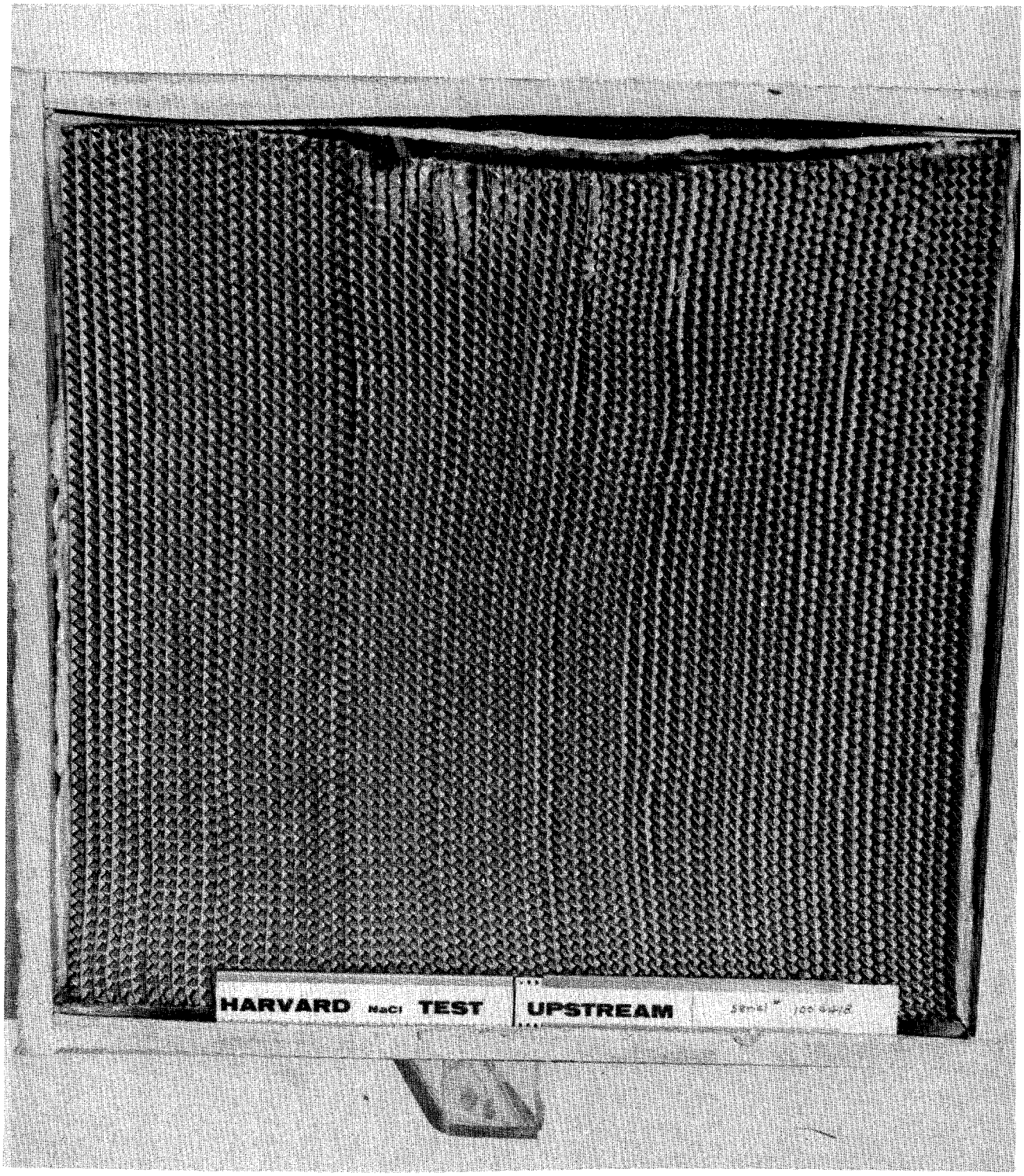

FIGURE IIA. FRONT FACE OF 1,000 C.F.M. FILTER AFTER HEAT STRESS. (PHOTO. COURTESY LAWRENCE LIVERMORE LAB.)

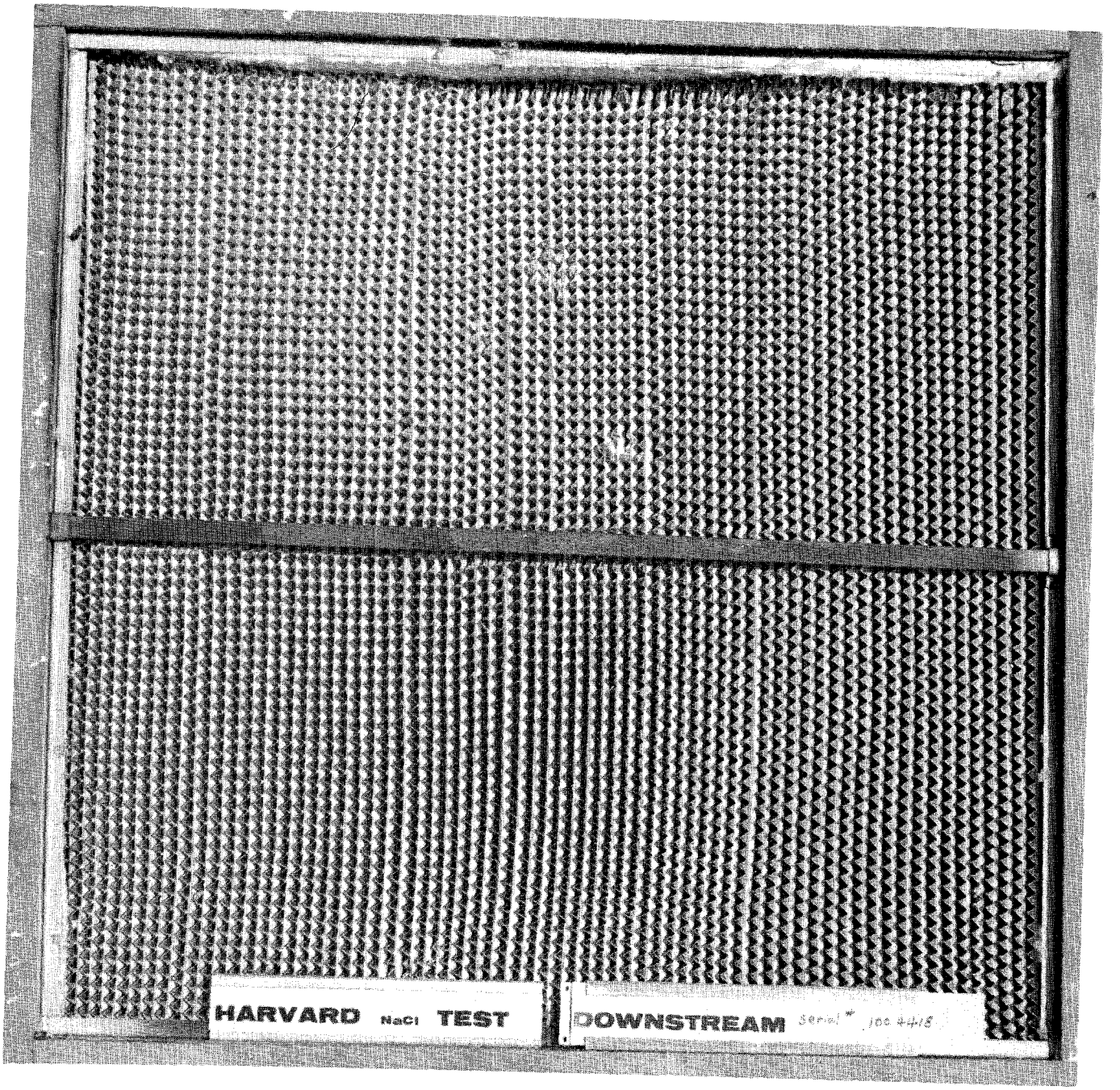

FIGURE IIB. REAR FACE OF 1,000 C.F.M. FILTER AFTER HEAT STRESS. (PHOTO. COURTESY LAWRENCE LIVERMORE LAB.)

4. Boyne, L., Dyment, J., and Thomason, I.D., "Generation of a Sodium Chloride Aerosol for Inplace Testing of Filters", (draft) Atomic Weapons-Research Establishment, Aldermaston, Berkshire, England (October, 1971).

5. Mitchell, R. N., Bevis, D. A., and E. C. Hyatt, "Comparison of Respirator Filter Penetration by Dioctyl Phthalate and Sodium Chloride", American Industrial Hygiene Association Journal, Vol. 32, pp. 357-364 (June, 1971).

6. Ferber, B. I., Brenenborg, F. J., and Rhode, A., "Respirator Filter Penetration Using Sodium Chloride Aerosol, United States Department of the Interior, Bureau of Mines, RI 7403 (June, 1970).

7. White, P. A. F., and Smith, S. E., eds. High Efficiency Air Filtration, Butterworth & Co. (Publishers) Ltd., London (1964) p. 164.

8. S. E. Smith (personal communication to Humphrey Gilbert) (9 January 1963).

9. Daniels, Farrington, and Alberty, Robert A., Physical Chemistry, 2nd Ed., Jonn Wiley & Sons, Inc., New York (1961) p. 138.

The research reported in this paper was supported by an Air and Gas Cleaning Contract of the U.S. Atomic Energy Commission under Contract Number AT(11-1)3049 with Harvard University.

DISCUSSION

DORMAN: I carried out with Dyment some of the initial experiments on the penetration of glass fiber paper sheets at elevated temperatures. We took a paper which had no measureable penetration at room temperature and we found no measureable penetration as we raised the temperature of the sheet up to about 750 F. After that, we got a measureable penetration which we attributed to the vapor press. A few years ago, I took another glass fiber paper with a penetration of about 0.01% at room temperature and I raised the temperature of it gradually and measured the penetration at the higher temperatures. I found that the percentage penetration fell linearly with rise in temperature up to about 570 F. It fell from about 0.01% down to 0.001%. When it cooled there was no measureable deterioration in its performance. Tomorrow, I hope to talk a little more about sodium chloride testing and perhaps we will change the color of the spectrum from a jaundiced view to a somewhat rosier one!

FIRST: Thank you, Mr. Dorman. I have been reading your most recent paper on this subject and I know that you speak as a foremost expert on sodium chloride testing.

BURCHSTED: When you said "brief exposure", how brief is "brief"?

FIRST: A matter of a few minutes; the time of exposure has been given in the Tables. In practice, we would generate the aerosol in an auxiliary duct, get the test tunnel up to temperature, run the aerosol through the filter long enough to get a test, and then switch the aerosol stream back to the auxiliary duct. The reason for this procedure was to avoid loading the filter with salt as accumulation of salt particles in the filter would cause efficiency to rise. Therefore, we tried to avoid long exposure to salt until after we had determined efficiency.

BURCHSTED: I would like to note, too, that what you have shown here tends to confirm what I reported at the 1968 IAEA Conference concerning deterioration, under heat, of media and the adhesives that hold the filters together.

JONAS: Was any correction made for the change in temperature; that is, the volume expansion of the aerosol going through, or increase in diffusivity to account for the difference in the penetration?

FIRST: I didn't bring this point up, but it is a very interesting one. When one performs comparative tests over a wide range of temperatures, a decision must be made to operate at constant velocity or at constant gas mass rate. We did both: the

heat-shrunk quartz papers were tested at constant mass flow; the commercial filters, at constant volumetric flow.

STEINBERG: Do you have any idea what the concentration was upstream of the salt?

FIRST: This is noted in the Tables in the paper.

STEINBERG: Is there any possibility that you might have been getting more salt through on each subsequent test, because, after all, you were picking up quite a bit on the filter itself.

FIRST: We checked this be passing clean air, at temperature, through filters after salt testing and noting whether or not we were able to detect salt penetration. In tests made solely for measureing salt penetration, we were not able to detect penetration when there were no salt particles in the entering air.